

**UNCLASSIFIED**

---

---

**AD 276 282**

*Reproduced  
by the*

**ARMED SERVICES TECHNICAL INFORMATION AGENCY  
ARLINGTON HALL STATION  
ARLINGTON 12, VIRGINIA**



---

---

**UNCLASSIFIED**

Best Available Copy

NOTICE: When government or other drawings, specifications or other data are used for any purpose other than in connection with a definitely related government procurement operation, the U. S. Government thereby incurs no responsibility, nor any obligation whatsoever; and the fact that the Government may have formulated, furnished, or in any way supplied the said drawings, specifications, or other data is not to be regarded by implication or otherwise as in any manner licensing the holder or any other person or corporation, or conveying any rights or permission to manufacture, use or sell any patented invention that may in any way be related thereto.

Best Available Copy

ORDNANCE CORPS  
DIAMOND ORDNANCE FUZE LABORATORIES  
WASHINGTON 25, D. C.

IN REPLY  
REFER TO:

AMXDO-RBA

7 Sept 1962

AD 276 282

TO: Recipients of DOFL Report No. TR-1031  
FROM: W. H. Pepper/AMXDO-RBA  
SUBJECT: "A MINIATURE AUTOMATIC DIRECTION FINDER," H. B. Smith, Jr.,  
J. A. Kaiser, W. H. Pepper and J. Little. dtd 14 May 1962.

The following corrections and additions should be made in the above-referenced report:

Page 7, 6th line from bottom: Change "90°" to "180°" to read "...shifting the null 180°."

Pages 9, 10 and 12; tables 1, 2, and figure 4: Interchange "A" and "B".

Page 9, table 1: Add minus sign before first parenthesis in arm "D" to read "D  $-(-\alpha \sin \dots$ "

Pages 10 and 16, figures 3 and 7: Interchange "E" and "F".

Page 14, figure 6 (upper-right corner): Change " $E\phi = 270^\circ$ " to read " $F\phi = 270^\circ$ ."

Best Available Copy

R-138

CATALOGED BY ASTIA  
AS AD NO. 276282

**276 282**

**TR-1031**

**A MINIATURE AUTOMATIC DIRECTION FINDER**

**H.B. Smith, Jr.**

**J. A. Kaiser**

**W. H. Pepper**

**J. Little**

**14 May 1962**

APR 1962



**DIAMOND ORDNANCE FUZE LABORATORIES**

**ORDNANCE CORPS DEPARTMENT OF THE ARMY**

WASHINGTON, D.C.

**Best Available Copy**

## DIAMOND ORDNANCE FUZE LABORATORIES

Robert W. McEvoy  
Lt Col, Ord Corps  
Commanding

B. M. Horton  
Technical Director

The Diamond Ordnance Fuze Laboratories is a Class II research, development and engineering installation of the U.S. Army located in Washington, D.C. Originally established in September 1953, under the Ordnance Corps, the Diamond Ordnance Fuze Laboratories serves as the Ordnance Corps electronics laboratory, specializing in the following areas:

(1) To perform research, development, and engineering on systems for automatically detecting targets of military significance, for performing local target evaluation, for accomplishing safing and arming functions, and for providing initiation signals in a manner to maximize weapons effectiveness.

(2) To perform the necessary research, development, and engineering on components, subsystems, and systems of the type referred to in Item (1) to achieve maximum immunity of such systems to the conditions prevalent in a battlefield environment.

(3) To conduct a research program in fluid amplification for military applications.

(4) To conduct instrumentation research and development related to the above.

(5) To conduct basic research in the various required scientific fields related to the above.

In addition to its major facility, DOFL operates a field test area located at Blossom Point, Maryland, and the Diamond Ordnance Radiation Facility at the Forest Glen Annex of the Walter Reed Army Medical Center.

The findings in this report are not to be construed as an official Department of the Army position.

Best Available Copy

**DIAMOND ORDNANCE FUZE LABORATORIES**  
**ORDNANCE CORPS**                      **WASHINGTON 25, D. C.**

DA-SN06.01.013  
ONS-8210.11.17500  
DOFL Proj. 26100

TR-1031

14 May 1962

**A MINIATURE AUTOMATIC DIRECTION FINDER**

H. B. Smith, Jr.

J. A. Kaiser

W. H. Pepper

J. Little

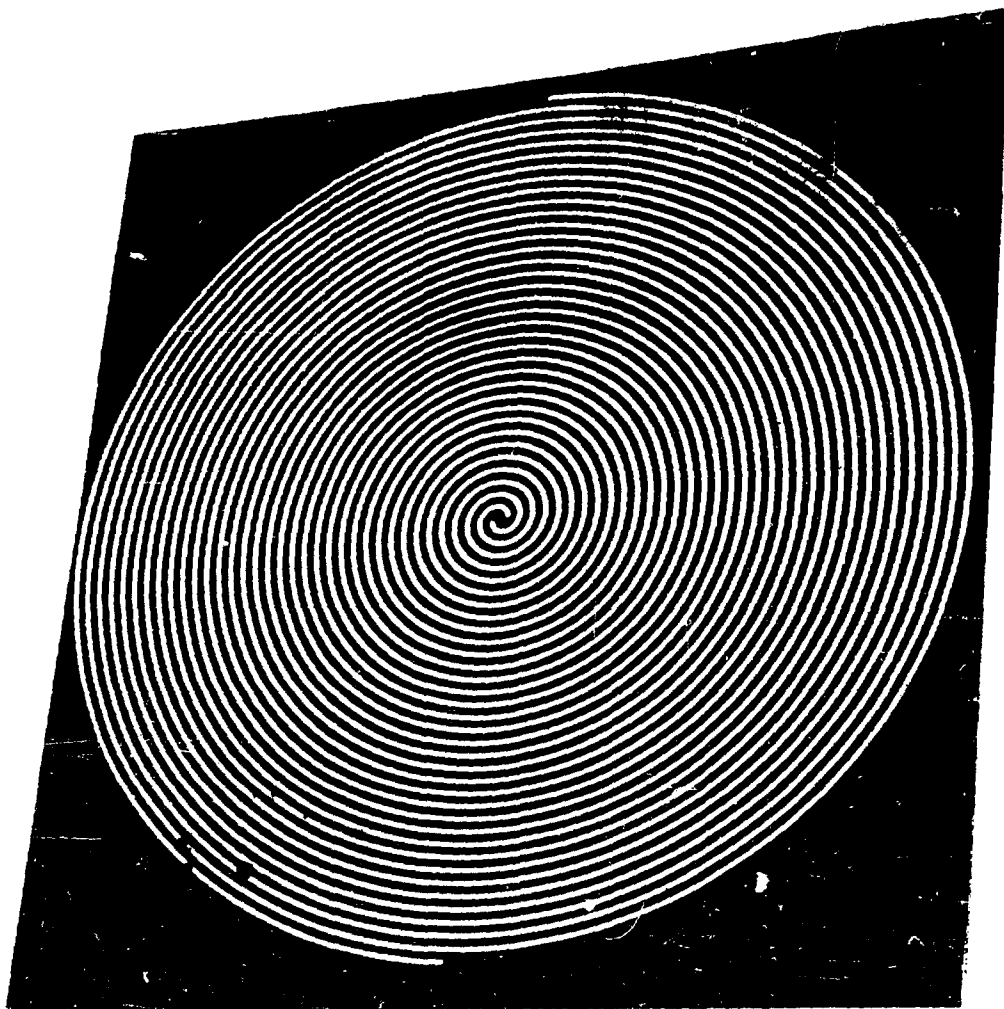
FOR THE COMMANDER:  
APPROVED BY



H. Sommer  
Chief, Laboratory 200



Qualified requesters may obtain copies of this report from ASTIA.



439 62

Frontispiece. Spiral Array.

## CONTENTS

	Page No.
ABSTRACT. . . . .	5
1. INTRODUCTION . . . . .	5
2. THEORETICAL DEVELOPMENT. . . . .	6
3. EXPERIMENTAL PROCEDURE . . . . .	16
4. CONCLUSIONS AND RECOMMENDATIONS. . . . .	31
APPENDIX A. . . . .	33

## ILLUSTRATIONS

Frontispiece	Spiral array.
Figure 1.	Ring network
Figure 2.	Spiral array phasing diagrams
Figure 3.	Direction finder network
Figure 4.	Theoretical detected signal in arms A and B as a function of elevation angle.
Figure 5.	Theoretical detected signal in arms C, D, E, F as a function of elevation angle, for $\phi = \pi/4$ .
Figure 6.	Theoretical detected signal in arms C, D, E, F as a function of elevation angle, for $\phi = 0, \pi/2, \pi, 3\pi/2$
Figure 7.	Experimental direction finder.
Figure 8.	Azimuthal plots of C, D, E, F for $\theta = 5^\circ$ .
Figure 9.	Azimuthal plots of C, D, E, F for $\theta = 10^\circ$ .
Figure 10.	Azimuthal plots of C, D, E, F for $\theta = 15^\circ$ .
Figure 11.	Azimuthal plots of C, D, E, F for $\theta = 30^\circ$ .
Figure 12.	Azimuthal plots of C, D, E, F for $\theta = 45^\circ$ .
Figure 13.	Azimuthal plots of C, D, E, F for $\theta = 60^\circ$ .
Figure 14.	Azimuthal plots of C, D, E, F for $\theta = 75^\circ$ .
Figure 15.	Azimuthal plots of A and B for $\theta = 5^\circ$ .
Figure 16.	Azimuthal plots of A and B for $\theta = 10^\circ$ .
Figure 17.	Azimuthal plots of A and B for $\theta = 15^\circ$ .
Figure 18.	Azimuthal plots of A and B for $\theta = 30^\circ$ .
Figure 19.	Azimuthal plots of A and B for $\theta = 45^\circ$ .

ILLUSTRATIONS (Cont'd)

- Figure 20. Azimuthal plots of A and B for  $\theta = 60^\circ$ .  
Figure 21. Azimuthal plots of A and B for  $\theta = 75^\circ$ .  
Figure A1. Theoretical Azimuthal Error for  $\gamma = 92^\circ$ .  
Figure A2. Theoretical Azimuthal Error for  $\gamma = 95^\circ$ .

## ABSTRACT

A miniaturized unambiguous direction finder with no moving parts is described. At a frequency of 1000 Mc, a complete system, consisting of a two-wire spiral antenna, with cavity backing, operating in the first two radiation modes can be built into a cylinder 10 in. in diameter and 3 in. deep. Direct scaling laws apply, so that at 3000 Mc, for example, the cylinder would be 5 in. in diameter and 1 1/2 in. deep. Since there are no moving parts, and printed-circuit techniques can be used, the total weight (excluding power supply and readout or display) will be less than 1/2 lb.

The pattern of this antenna array gives hemispheric coverage. The output, fed into an analog device, gives a determination of the elevation and azimuth of a received signal, with no ambiguities, in the hemisphere bounded by the plane of the spiral. The processing network consists of two 3-way power dividers and a pair of hybrids, which can be mounted on the back of the cavity by using strip-line techniques. An experimental version of the system has been built and preliminary data are presented.

## 1. INTRODUCTION

A miniature direction finder with no moving parts has been designed and constructed for guided missile application to meet the need for a compact, lightweight device with no directional ambiguities, to determine both elevation and azimuth. It uses a two-wire Archimedean<sup>1</sup> spiral antenna operating in the first two modes simultaneously. Although the antenna may also be used as a scanning device, discussion herein is limited to the direction finder.

The directional finder has not only the required deep null broadside for accurate null finding near the axis, but also the capability of uniquely determining the signal direction in terms of the conventional antenna spherical coordinate angles  $\theta$  and  $\phi$  in a wide cone about the antenna axis by using relative amplitudes of signals out of six terminals of a network. This network consists of two 3-way power dividers and two hybrid ring networks. By the theorem of reciprocity, if coherent signals are fed into the six output arms of the network, the direction of the main lobe of the antenna may be uniquely positioned by varying the relative amplitudes of the six signals. Further research will be required to increase the precision of the direction finder.

---

<sup>1</sup>Based on a spiral mode selector circuit for an Archimedean spiral array, DOFL Legal and Patent Service Office Docket No. 1091, J. A. Kaiser.

## 2. THEORETICAL DEVELOPMENT

To describe the manner in which the device functions, a spiral antenna as a radiator is considered first. A two-wire, self-complementary, Archimedean spiral antenna,<sup>1 2</sup> connected to terminals 5 and 6 of the ring network is fed from either terminal 1 or 2 as illustrated in figure 1. The diameter of the antenna must be at least  $2\lambda/\pi$  but less than  $3\lambda/\pi$ , where  $\lambda$  is the operational wavelength, so that the antenna will operate in the first two radiation modes only.

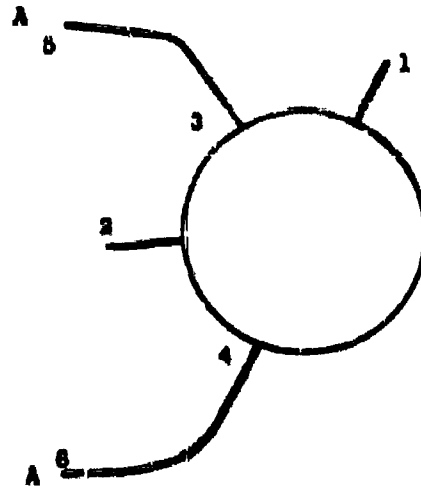


Figure 1. Ring network.

<sup>1</sup>J. A. Kaiser, "The Archimedean Two-Wire Spiral Antenna" IRE PGAP, Vol AP-8 (1960) p 312.

<sup>2</sup>J. A. Kaiser, "Flat Archimedean Spiral Antenna, Principles and Application," DOFL TR-726, 15 Aug 59.

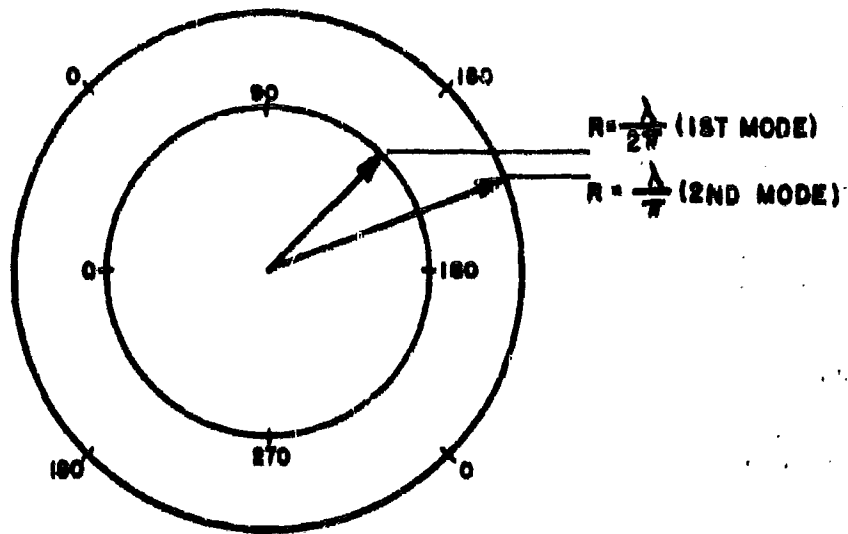
Assume that a radio frequency signal is applied to terminal 1 of the ring network. The energy of this signal divides equally as it enters the ring and emerges from the network at terminals 3 and 4 with equal amplitudes, but  $180^\circ$  out of phase. Consider that the lines from 3 to 5 and 4 to 6 are of equal length so that there is no relative phase shift of the two signals entering the terminals of the antenna. In the vicinity of the center of the antenna the currents are out of phase; for this reason little radiation occurs. As the currents proceed away from the center, the relative phase is shifted because of the difference in path lengths along the two spiral filaments. When the difference in path lengths between adjacent conductors is  $\lambda/2$ , the currents in these conductors are in phase and the radiation vectors add. Even for fairly coarse Archimedean spiral antennas, the difference in path length of  $\lambda/2$  can be approximated as occurring in a thin annulus of radius  $\lambda/2\pi$ . At some point in this circular region, the currents in adjacent filaments will be in phase with the currents entering into terminal 1. Using this as a reference point, one can establish a relative phase diagram of the currents about this  $\lambda/2\pi$  radius circle. [See inner ring in (A) of fig. 2] This mode of operation is called the first radiation mode.

Similarly, if a signal is applied to terminal 2 of the network shown in figure 1, the currents entering the antenna are in phase and of equal amplitude, and the radiation vectors will add on the  $\lambda/\pi$  radius circle. Again one can establish the relative phase diagram [outer ring in (A) of fig. 2] with this mode of operation, called the second radiation mode. Note, however, that the "O" phase of the second mode may or may not lie on the same radius as the "O" phase point of the first radiation mode.

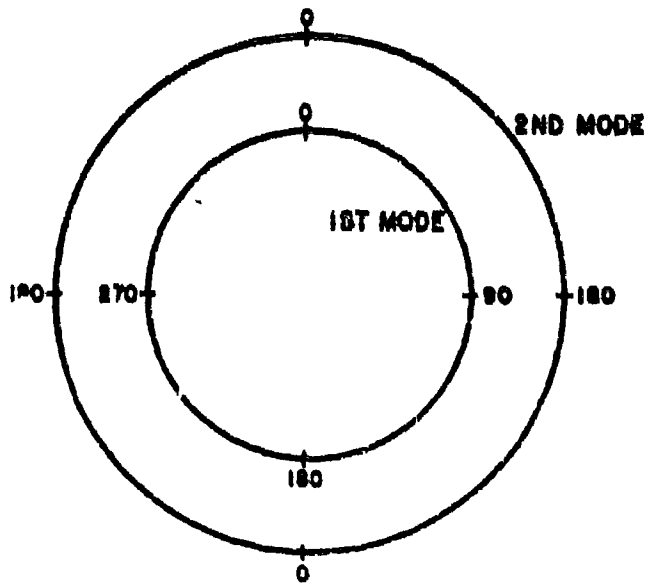
The phase of the currents establish the phase of the radiation fields. At some angle  $\phi$ , the radiation fields of the first mode and the second mode are in phase. This direction is referred to as  $\phi = 0$ , and the phase diagram is redrawn as shown in (B) of figure 2, indicating the direction of in-phase fields as "O" - "O".

If an rf signal is fed into both terminals 1 and 2, both modes will be excited simultaneously. If these signals are in phase, the radiation field will be such that the radiation vectors of the first and second mode will add in the  $\phi = 0^\circ$  direction and cancel in the  $\phi = 180^\circ$  direction, thus forming a null in the  $\phi = 180^\circ$  direction. If the phase into terminal 1 is shifted by  $180^\circ$ , the first mode is rotated through  $180^\circ$ , shifting the null to the direction of  $\phi = 0^\circ$ . If the signal into terminal 2 is shifted by  $180^\circ$ , the physical rotation of the second mode is  $90^\circ$ , shifting the null  $90^\circ$ . By the theorem of reciprocity, if the antenna is used as a receiver, the phase of the signals out of terminals 1 and 2 can be used to determine the direction of the source.

The exact field equations for the spiral antenna operating in the first or second mode have not been derived. As an approximation, based on pattern measurements, the first mode antenna pattern can be



(A) RELATIVE PHASE DIAGRAM



(B) DIRECTION OF IN-PHASE FIELDS

Figure 2. Spiral array phasing diagrams.

represented by  $\beta \cos \theta e^{(j\phi + j\omega t)}$ , and the second mode by  $\alpha \sin \theta e^{(j2\phi + j\omega t)}$ , where  $\phi$  is defined in the range 0 to  $2\pi$ , and  $\theta$  is defined between 0 and  $\pi/2$ . These are in phase at  $\phi = 0$ , as required by the method of defining the radiation fields of the first and second modes. Also, if the crossover point of the relative gain patterns of the two modes occurs at  $\theta = \theta_0$ , then

$$\alpha \sin \theta_0 = \beta \cos \theta_0$$

Assume a signal received by the antenna from a direction  $(\theta, \phi)$ , fed into a network, shown in figure 3, consisting of two 3-way power dividers and two hybrid ring networks. The line lengths of the network are such that  $a = b$ ,  $c = d$ ,  $e = f + \lambda/4$ , where  $\lambda$  is the system design wavelength. The signals in the arms, before detection, are of the form shown in table 1.

Table 1. Antenna Signal Forms

A	$(2 \beta \cos \theta e^{j\phi}) e^{j\omega t}$	(first mode)
B	$(2 \alpha \sin \theta e^{j2\phi}) e^{j\omega t}$	(second mode)
C	$(\alpha \sin \theta e^{j2\phi} + \beta \cos \theta e^{j\phi}) e^{j\omega t}$	
D	$(-\alpha \sin \theta e^{j2\phi} + \beta \cos \theta e^{j\phi}) e^{j\omega t}$	
E	$(\alpha \sin \theta e^{j2\phi} + \beta \cos \theta e^{j\phi}) e^{j(\omega t - \pi/2)}$ $+ (-\alpha \sin \theta e^{j2\phi} + \beta \cos \theta e^{j\phi}) e^{j\omega t}$	
F	$(\alpha \sin \theta e^{j2\phi} + \beta \cos \theta e^{j\phi}) e^{j(\omega t - \pi/2)}$ $- (-\alpha \sin \theta e^{j2\phi} + \beta \cos \theta e^{j\phi}) e^{j\omega t}$	

After square law detection, these signals are of the form shown in table 2.

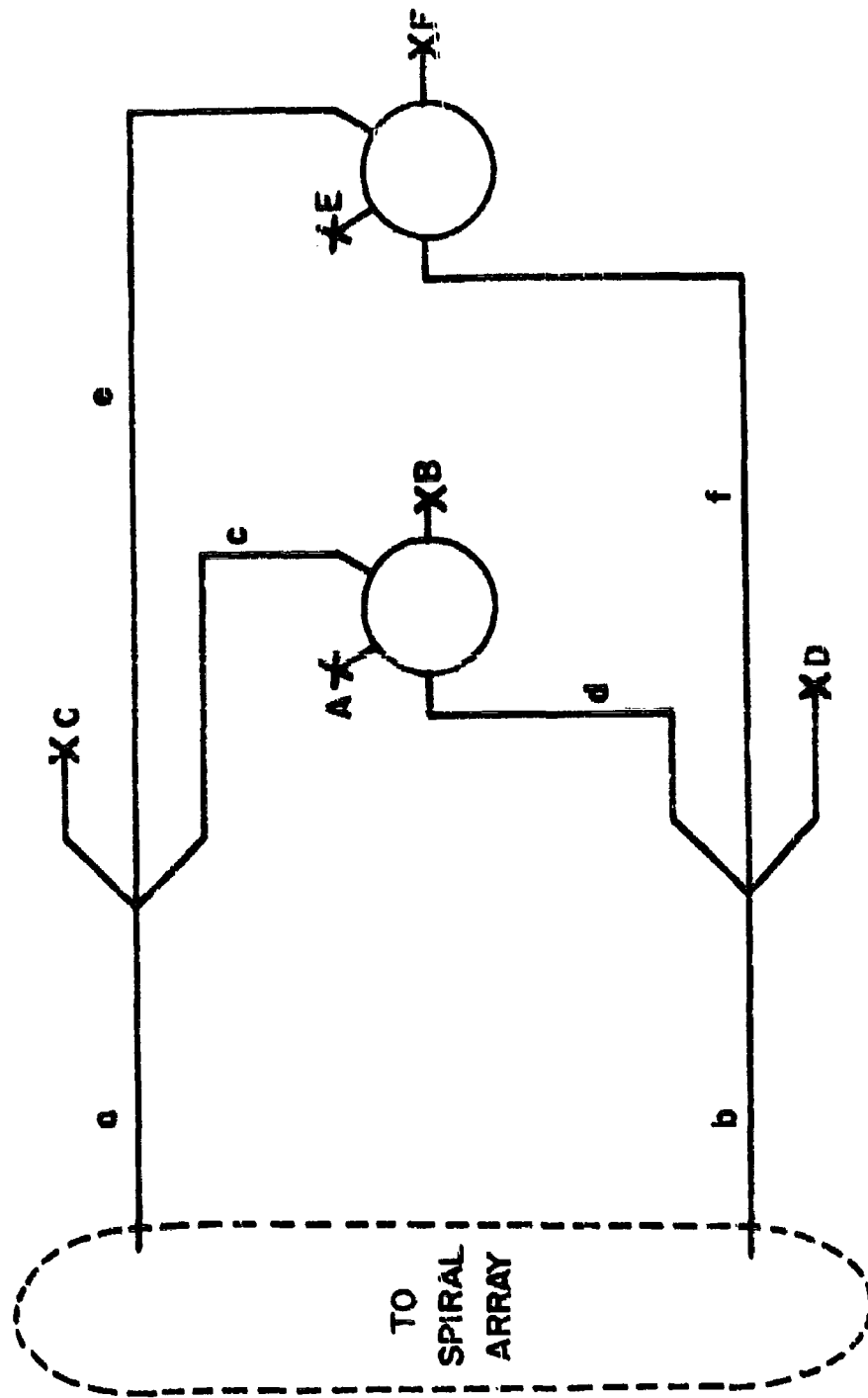


Figure 3. Direction finder network.

Table 2. Signal Forms After Square Law Detection

A	$\beta^2 \cos^2 \theta$
B	$\alpha^2 \sin^2 \theta$
C	$\alpha^2 \sin^2 \theta + \beta^2 \cos^2 \theta + 2 \alpha \beta \sin \theta \cos \theta \cos \phi$
D	$\alpha^2 \sin^2 \theta + \beta^2 \cos^2 \theta - 2 \alpha \beta \sin \theta \cos \theta \cos \phi$
E	$\alpha^2 \sin^2 \theta + \beta^2 \cos^2 \theta + 2 \alpha \beta \sin \theta \cos \theta \sin \phi$
F	$\alpha^2 \sin^2 \theta + \beta^2 \cos^2 \theta - 2 \alpha \beta \sin \theta \cos \theta \sin \phi$

It can be seen that the sum of the indications (power) in arms A and B is equal to the sum of the indications in arms C and D, and is also equal to the sum of the indications in arms E and F, which must be the case considering the method in which the power is split up. These six arms have signals that are apparently a function of four variables:  $\alpha$ ,  $\beta$ ,  $\theta$ , and  $\phi$ . However, since the products  $\alpha \sin \theta$  and  $\beta \cos \theta$  are the only way in which these parameters appear, the signals in the six arms can actually be expressed in terms of three variables:  $\alpha \sin \theta$ ,  $\beta \cos \theta$ , and  $\phi$ . Also, the detected signals in arms A and B are seen to be independent of  $\phi$ .

To find the direction from which an incident signal is coming, an algebraic function of the signals in arms, A, B, C, D, E, and F (for simplicity, the amplitude of the detected signal in an arm is represented by the name of the arm), combined with the knowledge of  $\theta$  (which can be set by calibration) is all that is necessary. By simple manipulation

$$\phi = \sin^{-1} \left[ \frac{E-F}{[(E-F)^2 + (C-D)^2]^{1/2}} \right] \quad (1)$$

and

$$\theta = \tan^{-1} \left[ \left( \frac{A}{B} \right)^{1/2} \tan \theta_0 \right]$$

Theoretical plots of the amplitudes of the detected signals as a function of variations in  $\theta$  and  $\phi$  are given in figures 4, 5, and 6. There are, of course many other relationships<sup>1</sup> that can be used to calculate

<sup>1</sup> A simpler relation for  $\phi$  would be  $\phi = \tan^{-1} \frac{(E-F)}{(C-D)}$  but this would be difficult to handle in the region in which  $C-D \rightarrow 0$ , in which case one could consider  $\phi = \cot^{-1} \frac{(C-D)}{(E-F)}$ .

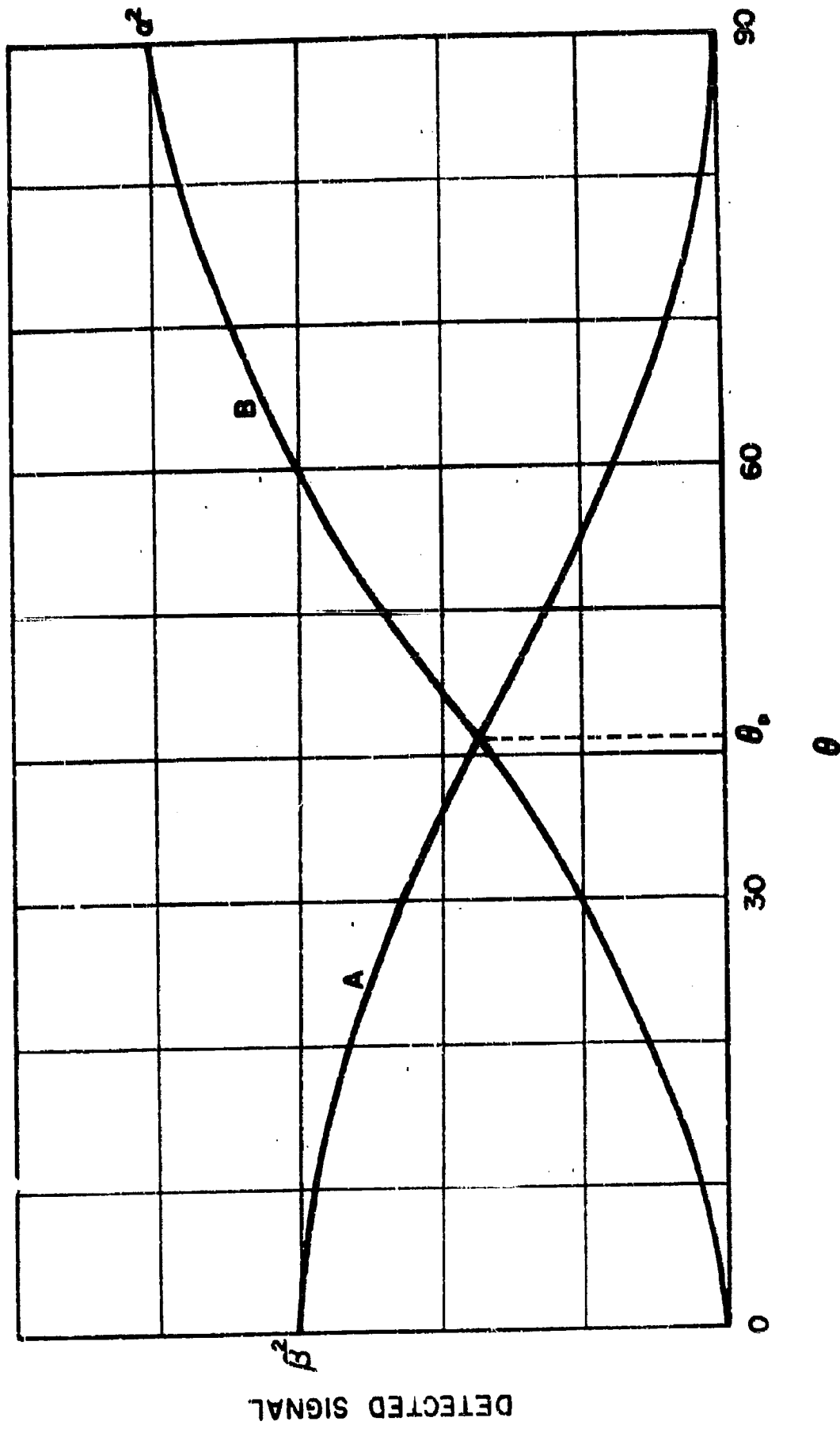


Figure 4. Theoretical detected signal in arms A and B as a function of elevation angle.

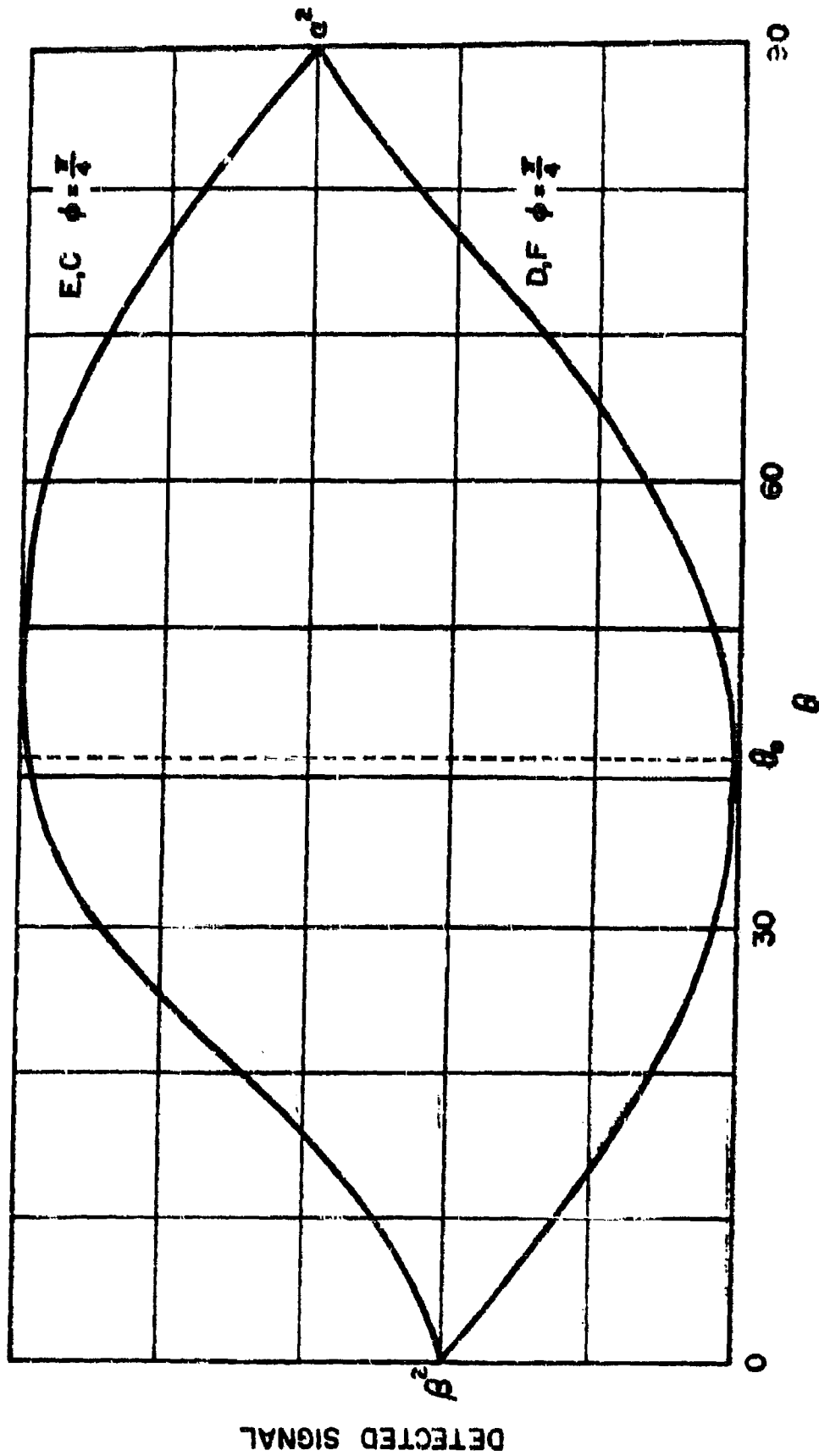


Figure 5. Theoretical detected signal in arms C, D, E, F as a function of elevation angle, for  $\phi$  equal to  $\pi/4$ .

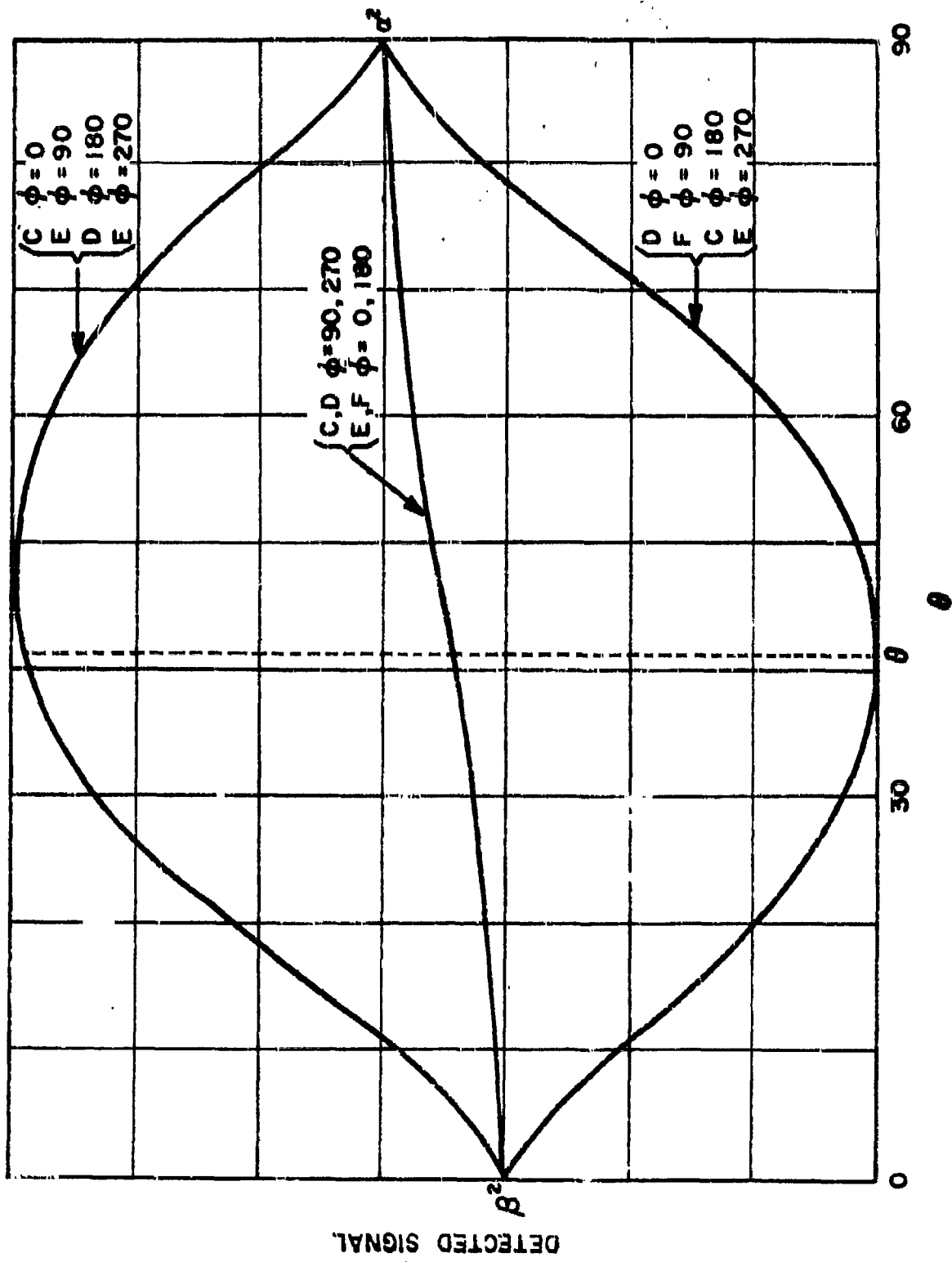


Figure 6. Theoretical detected signal in arms C, D, E, F as a function of elevation angle, for  $\phi, \pi/2, \pi, (3\pi)/2$ .

$\phi$  and  $\theta$ , and a study of the deviation of the actual first and second mode antenna patterns from the assumed relations might be useful in determining the probable deviation of the actual source direction from the calculated source direction.

From the redundancy in observations, it might seem that fewer detectors could be used to determine  $\theta$  and  $\phi$ . In this section it will be shown that, in general, this is not possible, but that under certain assumptions it might be possible to eliminate arms A and B (and thus replace the three-way power dividers with two-way power dividers) from the system.

$$\text{Let } \frac{1}{2} \left[ (C-D)^2 + (E-F)^2 \right]^{1/2} = K_1 = 2 \alpha \beta \sin \theta \cos \theta$$

Then

$$\begin{aligned} K_2 &= 1/2 (C + D) + K_1 = \alpha^2 \sin^2 \theta + \beta^2 \cos^2 \theta + 2 \alpha \beta \sin \theta \cos \theta \\ &= \left[ \alpha \sin \theta + \beta \cos \theta \right]^2 \end{aligned}$$

and, similarly

$$K_3 = 1/2 (C + D) - K_1 = \left[ \alpha \sin \theta - \beta \cos \theta \right]^2$$

Now, if it is known how  $\theta$  compares with  $\theta_0$ , that is, whether it is larger or smaller, then  $\theta$  can be found. This might be the case in a direction finder or homing device. For example, if  $\theta > \theta_0$ , then  $\alpha \sin \theta - \beta \cos \theta < 0$ , and

$$\theta = \tan^{-1} \left[ \frac{K_2^{1/2} - K_3^{1/2}}{K_2^{1/2} + K_3^{1/2}} \tan \theta_0 \right]$$

if  $\theta < \theta_0$ , then  $\alpha \sin \theta - \beta \cos \theta < 0$ , and

$$\theta = \tan^{-1} \left[ \frac{K_2^{1/2} - K_3^{1/2}}{K_2^{1/2} + K_3^{1/2}} \tan \theta_0 \right]$$

Thus, if it is known from which general direction (in elevation) the received signal is expected, four detectors can be used instead of six. Also, by adjusting the pattern gains in the first and second modes (i.e.,  $\alpha$  and  $\beta$ ),  $\theta_0$  can be controlled and thus give better control over the region from which signals are permissible. Making  $\theta_0$  near  $0^\circ$  or  $90^\circ$ , however, will introduce a large uncertainty in the calculated direction for a small measurement error.

### 3. EXPERIMENTAL PROCEDURE

A two-wire Archimedean spiral antenna  $2\lambda/\pi$  in diameter was mounted  $\lambda/4$  in front of a 24-in. square ground plane. This assembly was then mounted on a two-axis rotator. The two outputs of the antenna were fed into the networks illustrated in figure 7.

The antenna was mounted so that it could be rotated about its axis of symmetry ( $\Theta = 0$ ). The antenna was illuminated with a circularly polarized continuous wave signal at 1020 Mc. The terminals at A through F were all terminated in matched dummy loads, except for one that was terminated in a square law detector. The detected signal amplitudes at C, D, E, F were recorded as a function of  $\phi$  for  $\phi = 5^\circ, 10^\circ, 15^\circ, 30^\circ, 45^\circ, 60^\circ, 75^\circ$  (figures 8, 9, 10, 11, 12, 13, 14). The amplitudes at A and B were recorded as a function of  $\phi$  for the  $\Theta$ 's listed above (fig. 15, 16, 17, 18, 19, 20, and 21).

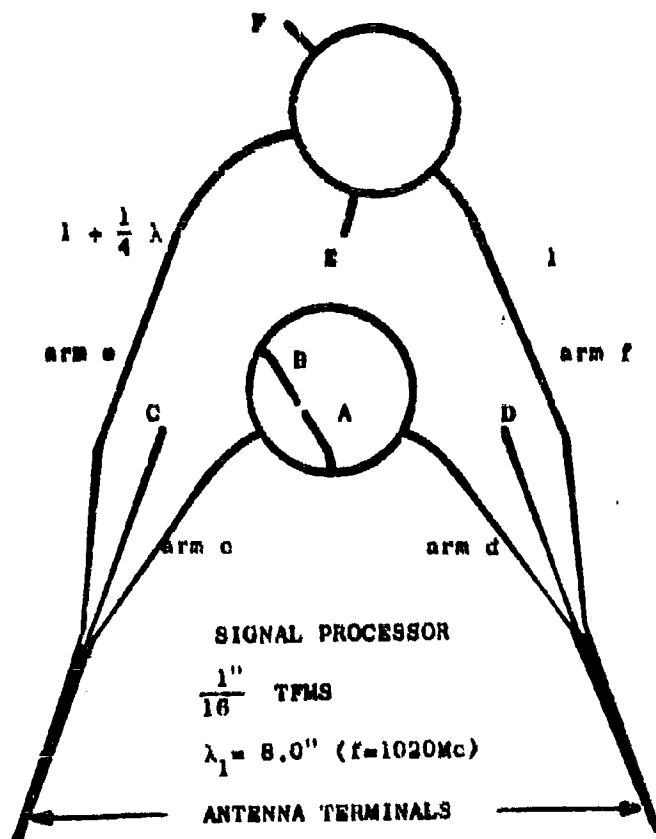
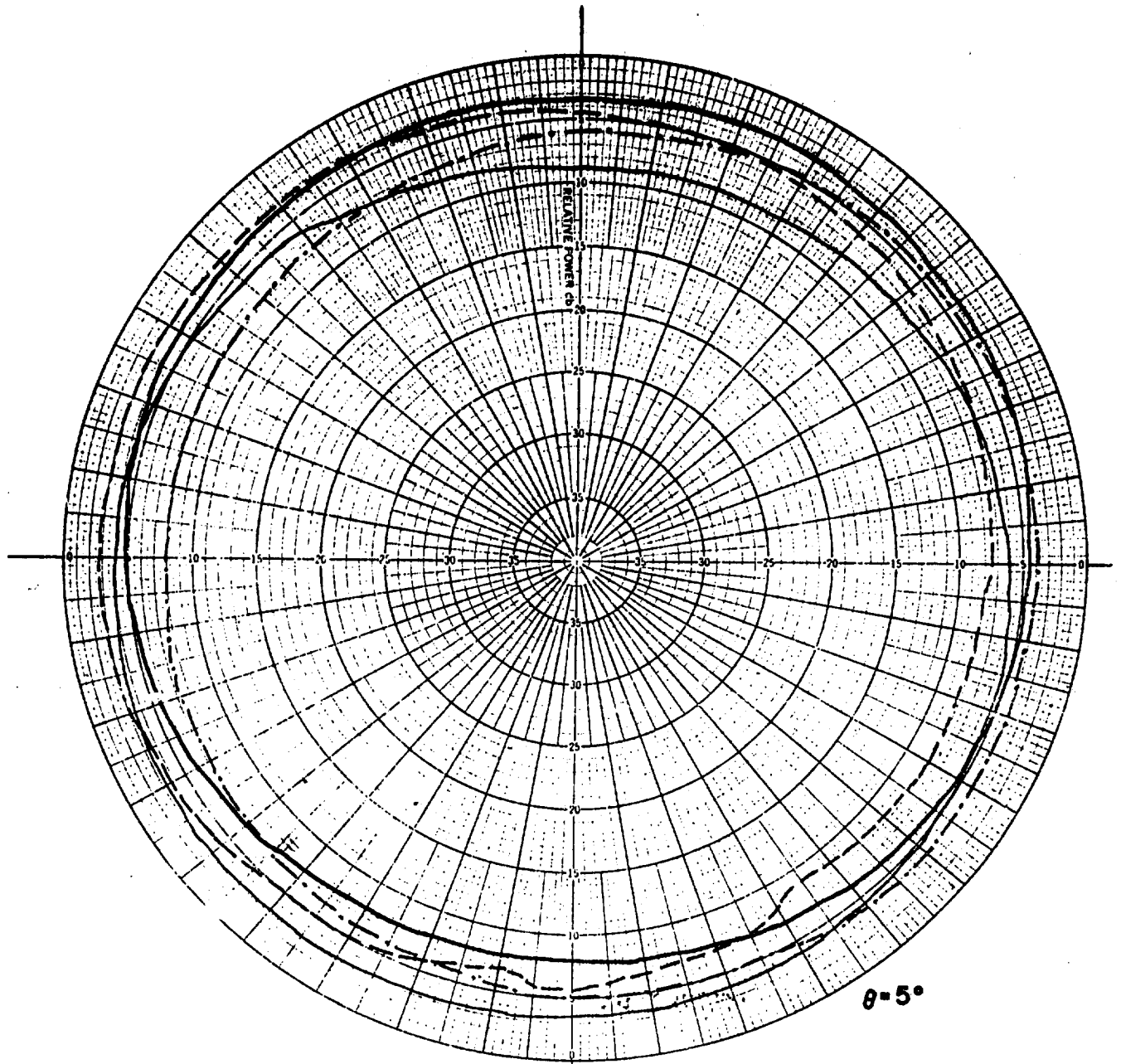


Figure 7. Experimental direction finder.



- ..... C
- D
- E
- F

$f_0 = 1022$  mcs -- LEFT CIRCULAR POLARIZATION

Figure 8. Azimuthal plots of C, D, E, F for  $\theta = 5^\circ$ .

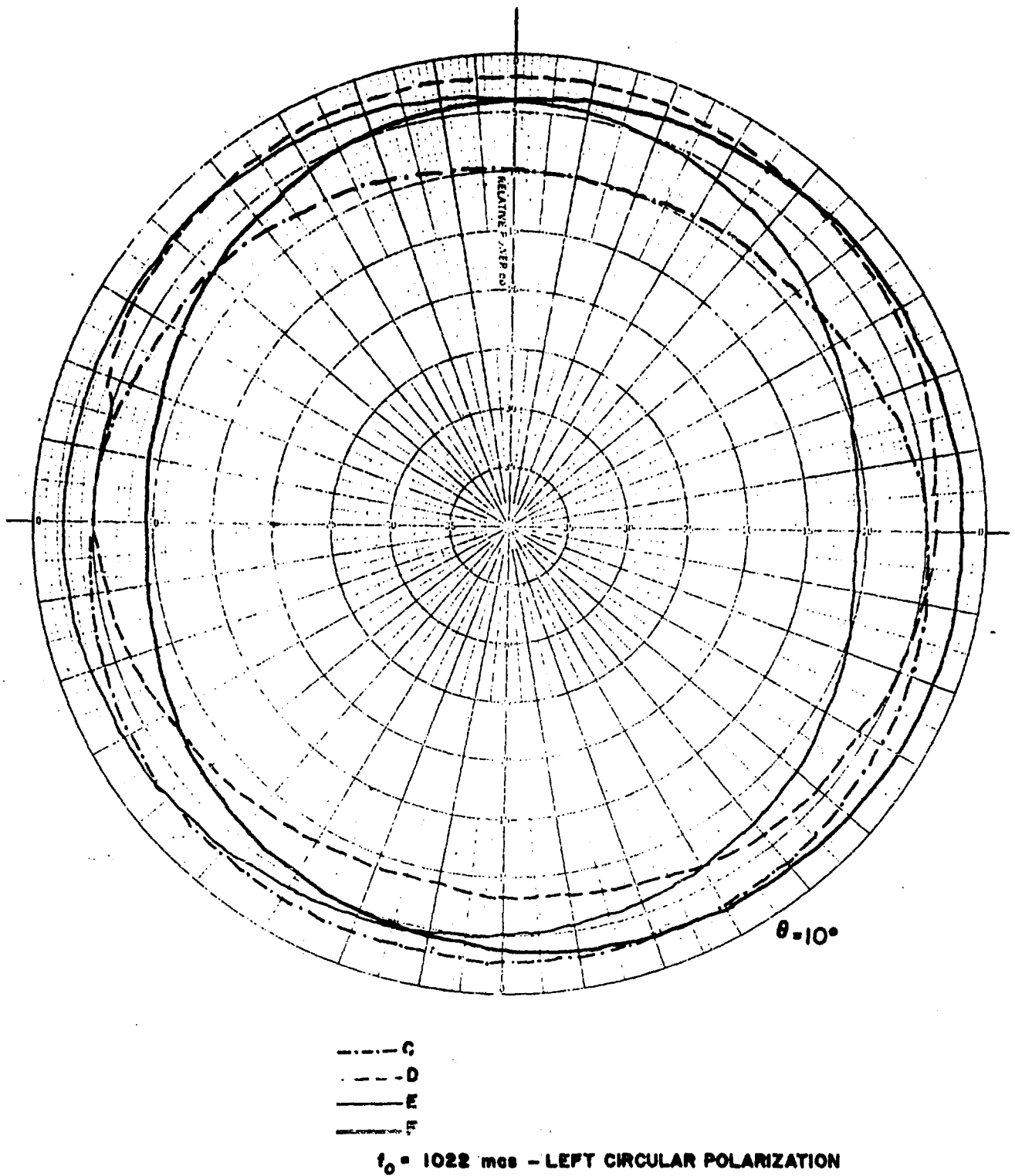
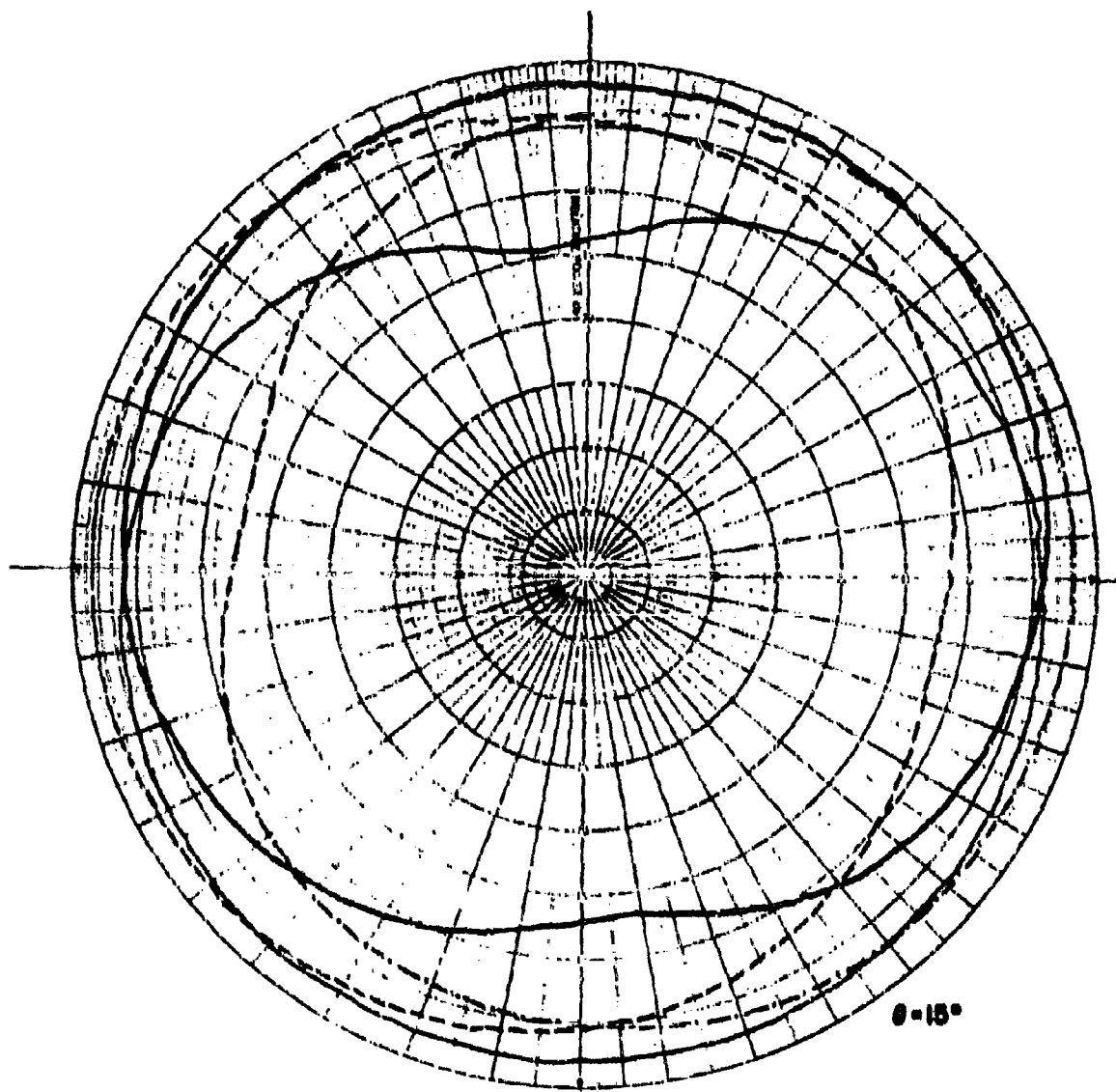


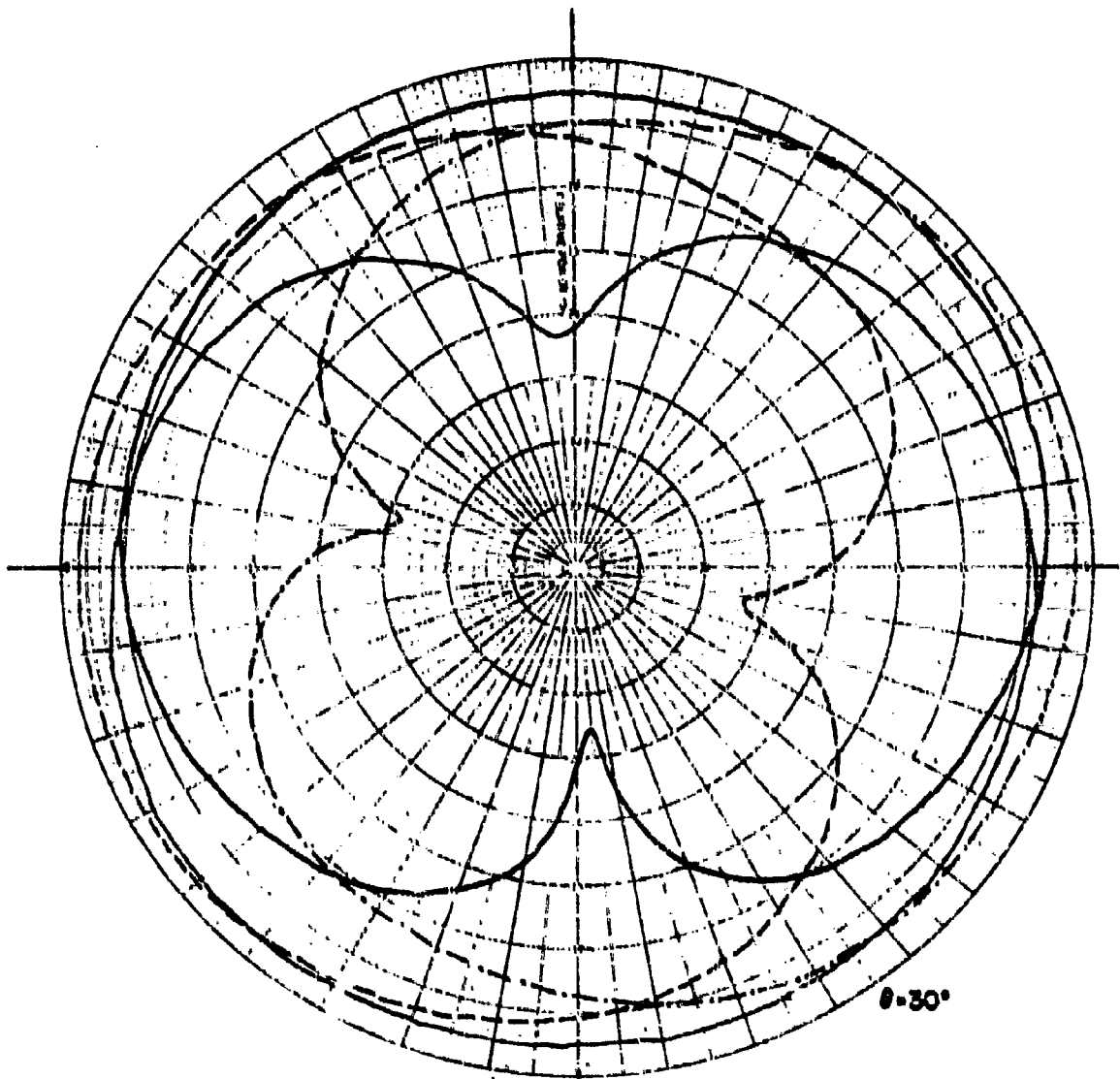
Figure 9. Azimuthal plots of C, D, E, F for  $\theta = 10^\circ$ .



..... C  
 - - - - D  
 \_\_\_\_\_ E  
 \_\_\_\_\_ F

$f_0 = 1022 \text{ mcs} - \text{LEFT CIRCULAR POLARIZATION}$

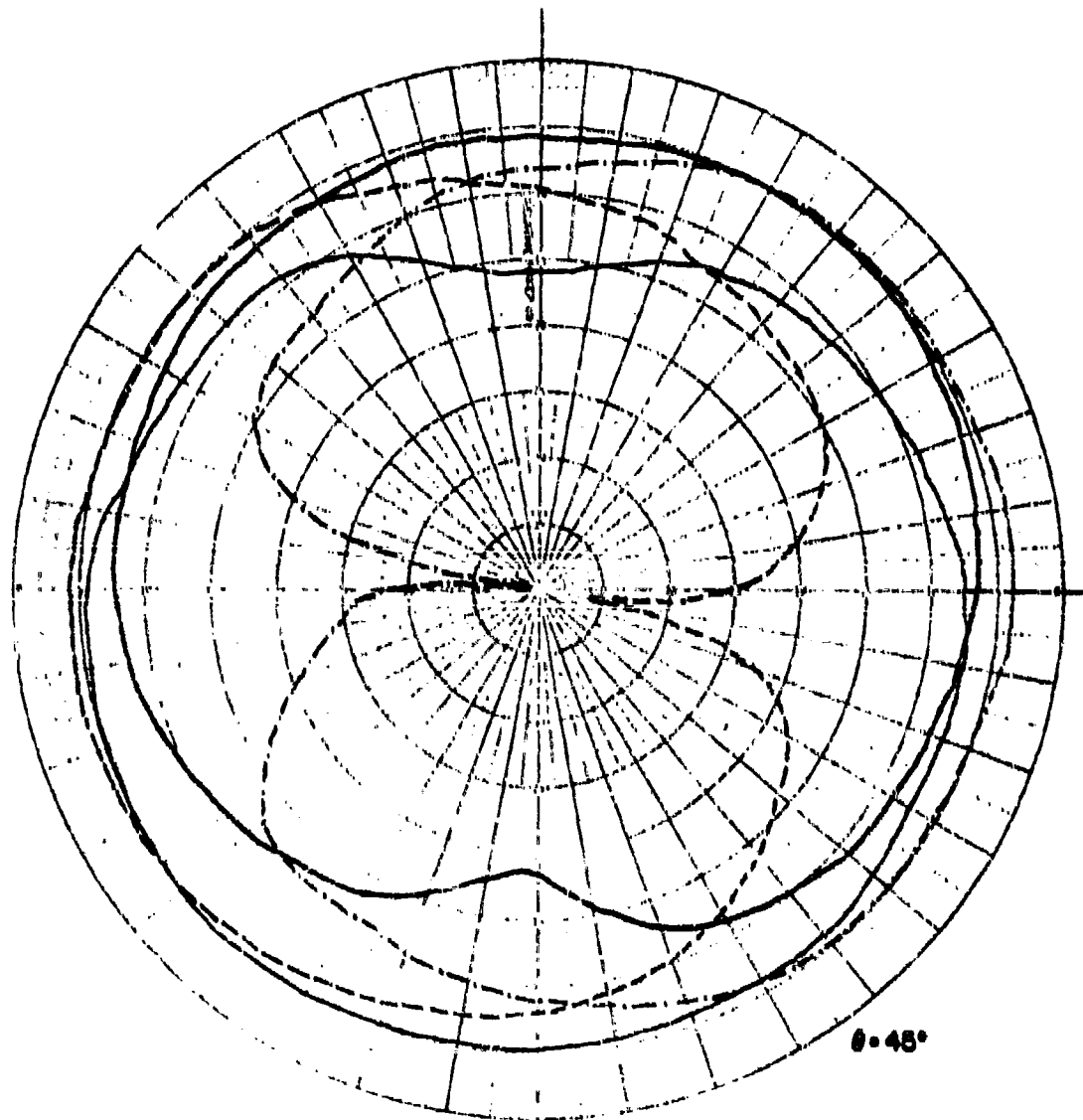
Figure 10. Azimuthal plots of C, D, E, F for  $\theta = 15^\circ$ .



..... C  
 - - - - D  
 ——— E  
 ——— F

$f_0 = 1028 \text{ mcs} - \text{LEFT CIRCULAR POLARIZATION}$

Figure 11. Azimuthal plots of C, D, E, F for  $\theta = 30^\circ$ .



····· G  
 - - - D  
 ——— E  
 ——— F

$\tau_0 = 1022 \text{ m}\mu\text{s}$  - LEFT CIRCULAR POLARIZATION

Figure 12. Azimuthal plots of G, D, E, F for  $\theta = 45^\circ$ .

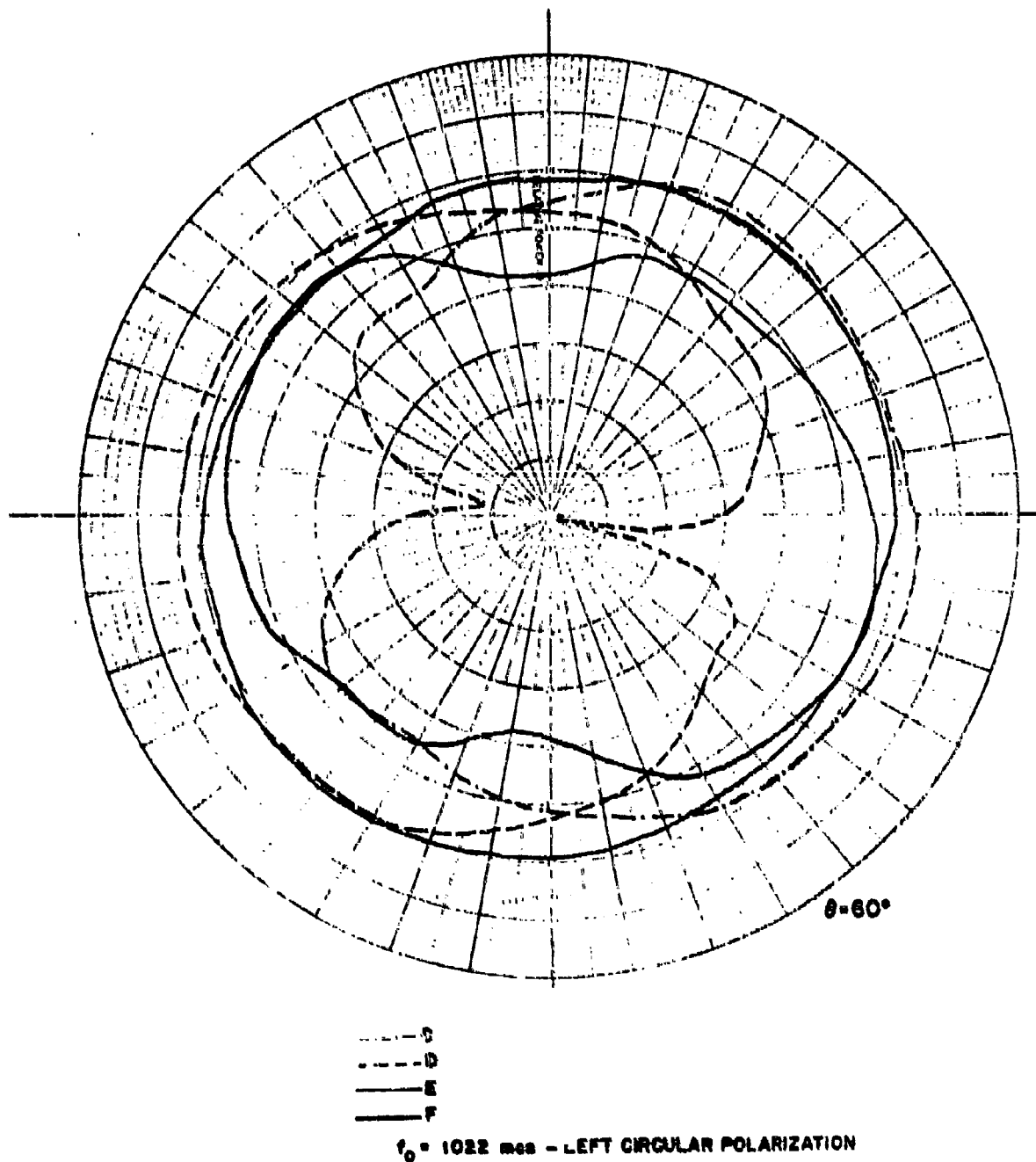
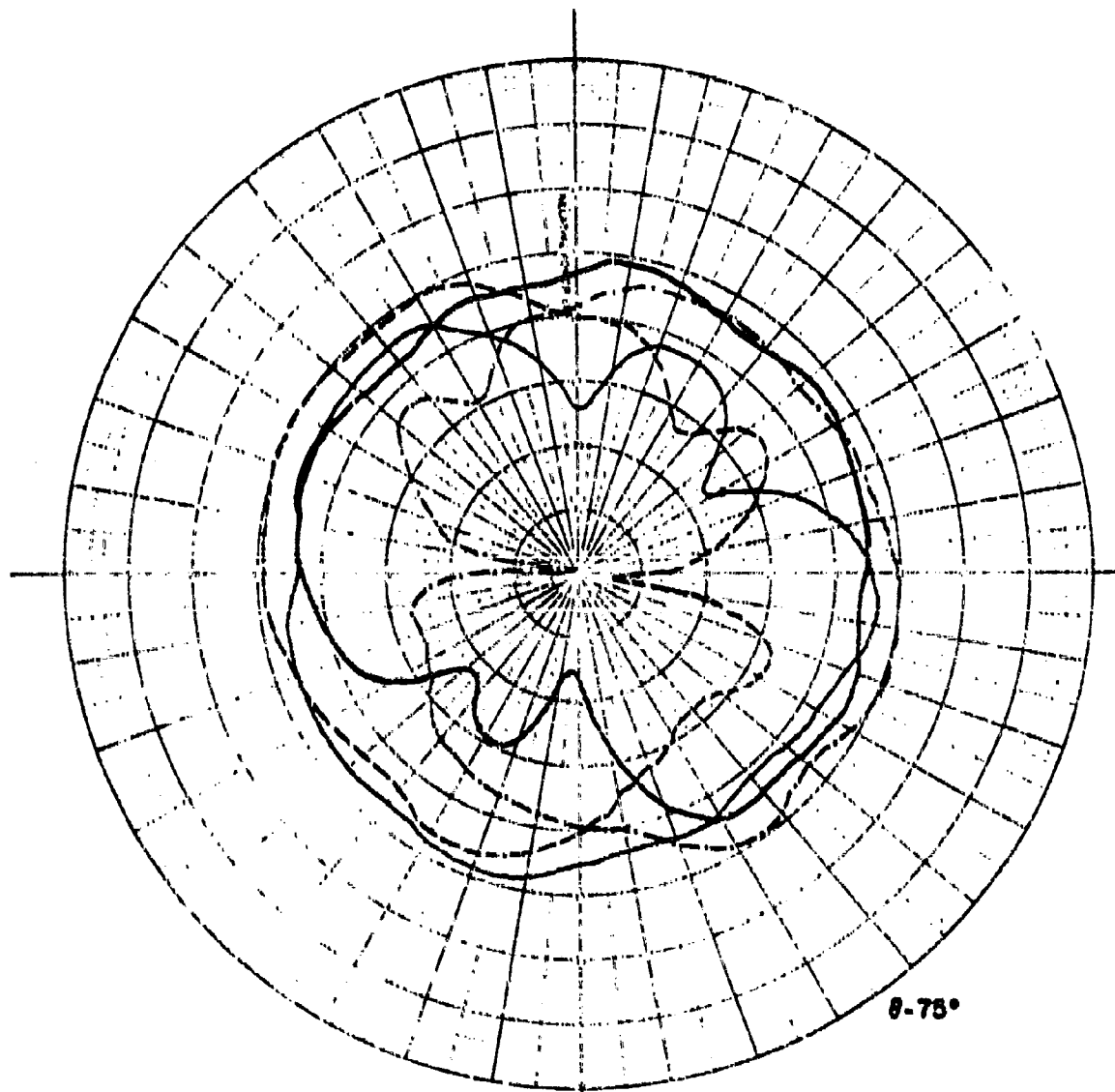


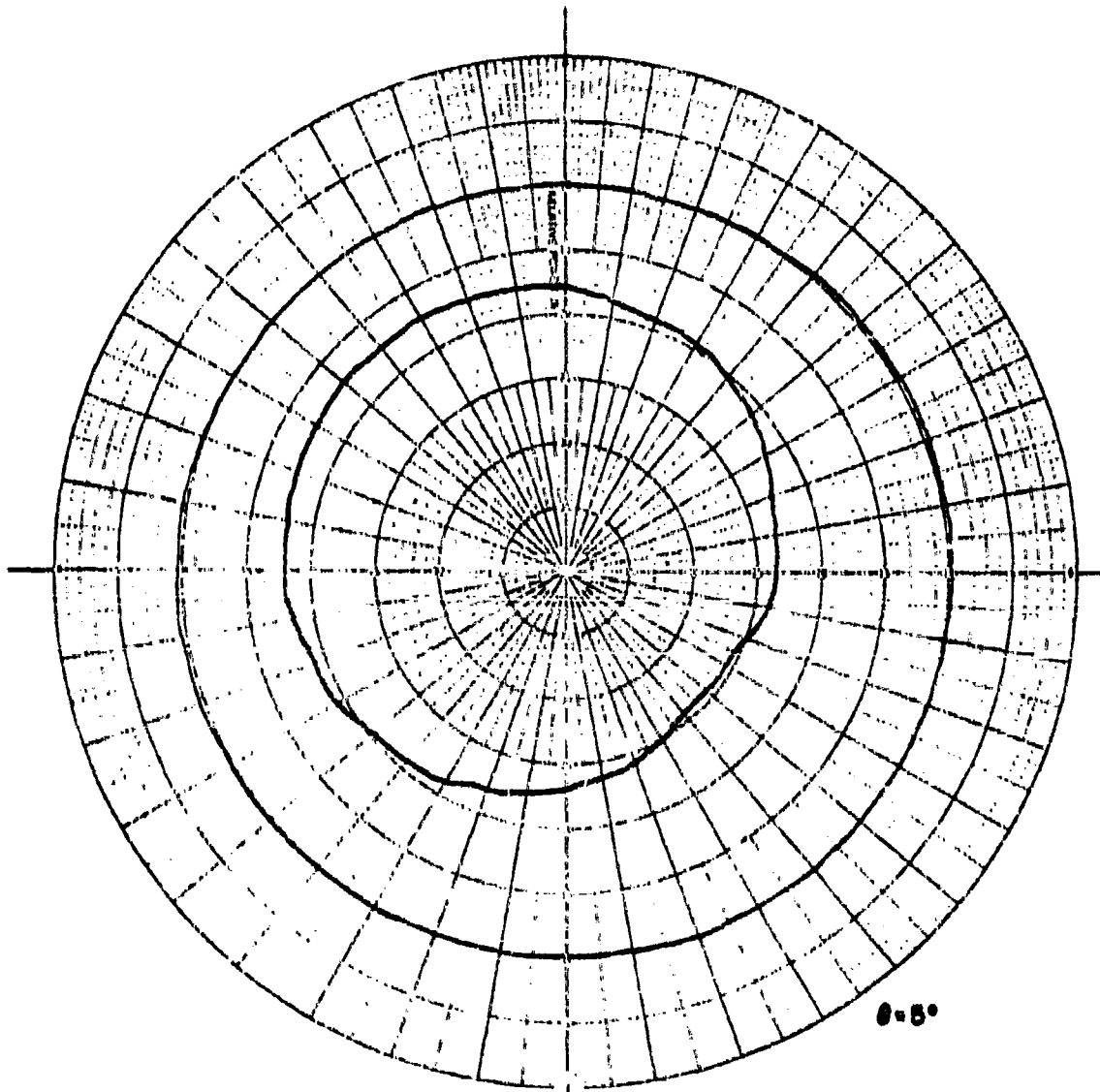
Figure 13. Azimuthal plots of C, D, E, F for  $\theta = 60^\circ$ .



.....C  
 - - - - D  
 ——— E  
 ——— F

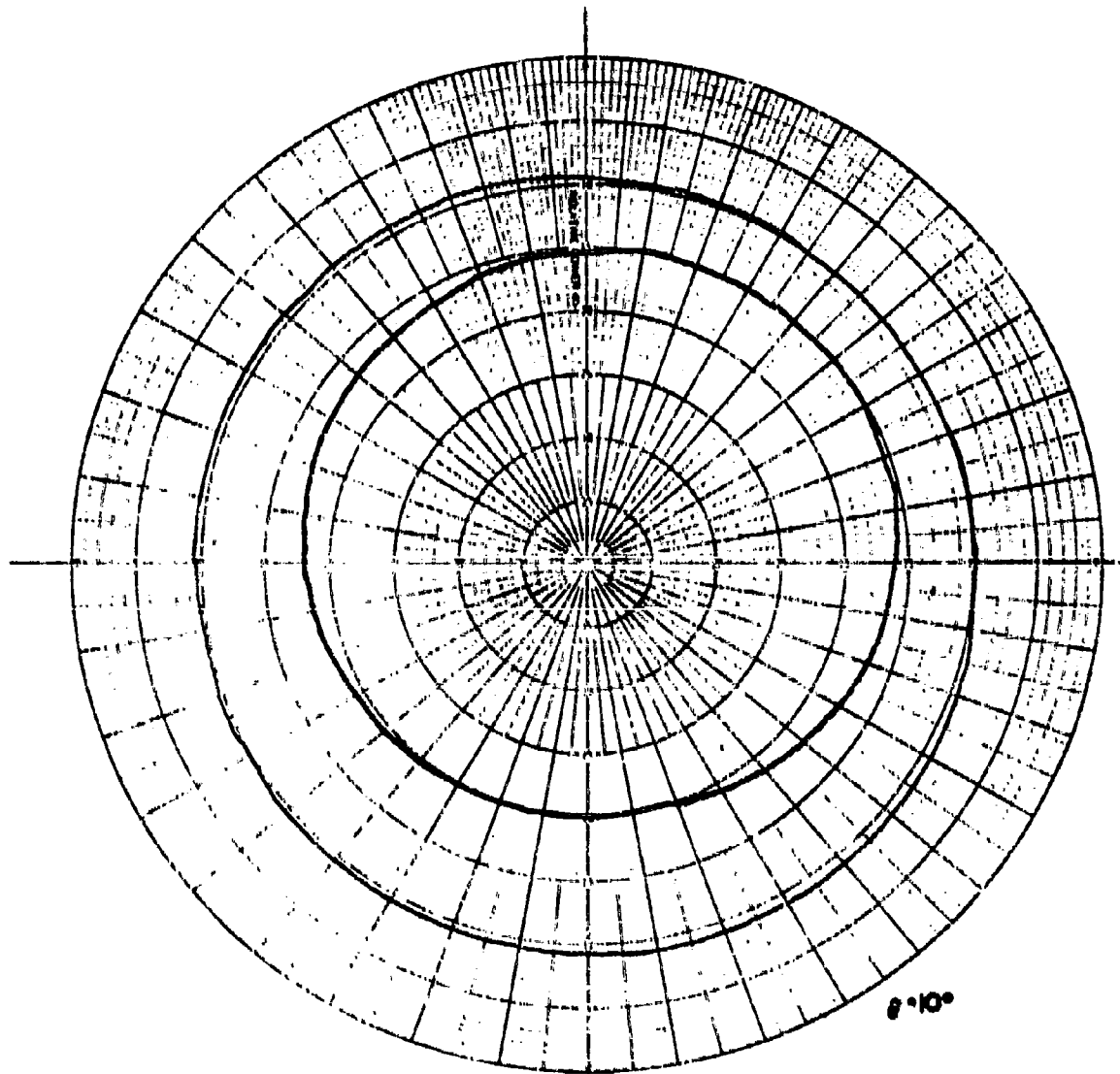
$f_0 = 1022 \text{ mcs} - \text{LEFT CIRCULAR POLARIZATION}$

Figure 14. Azimuthal plots of C, D, E, F for  $\theta = 75^\circ$ .



——— FIRST MODE PATTERN (A)  
 - - - SECOND MODE PATTERN (B)  
 $f_0 = 1022$  mcs - LEFT CIRCULAR POLARIZATION  
 THESE PATTERNS WERE RECORDED AT A GAIN  
 SETTING 10db BELOW THE OTHERS

Figure 16. Azimuthal plots of A and B for  $\theta = 5^\circ$ .

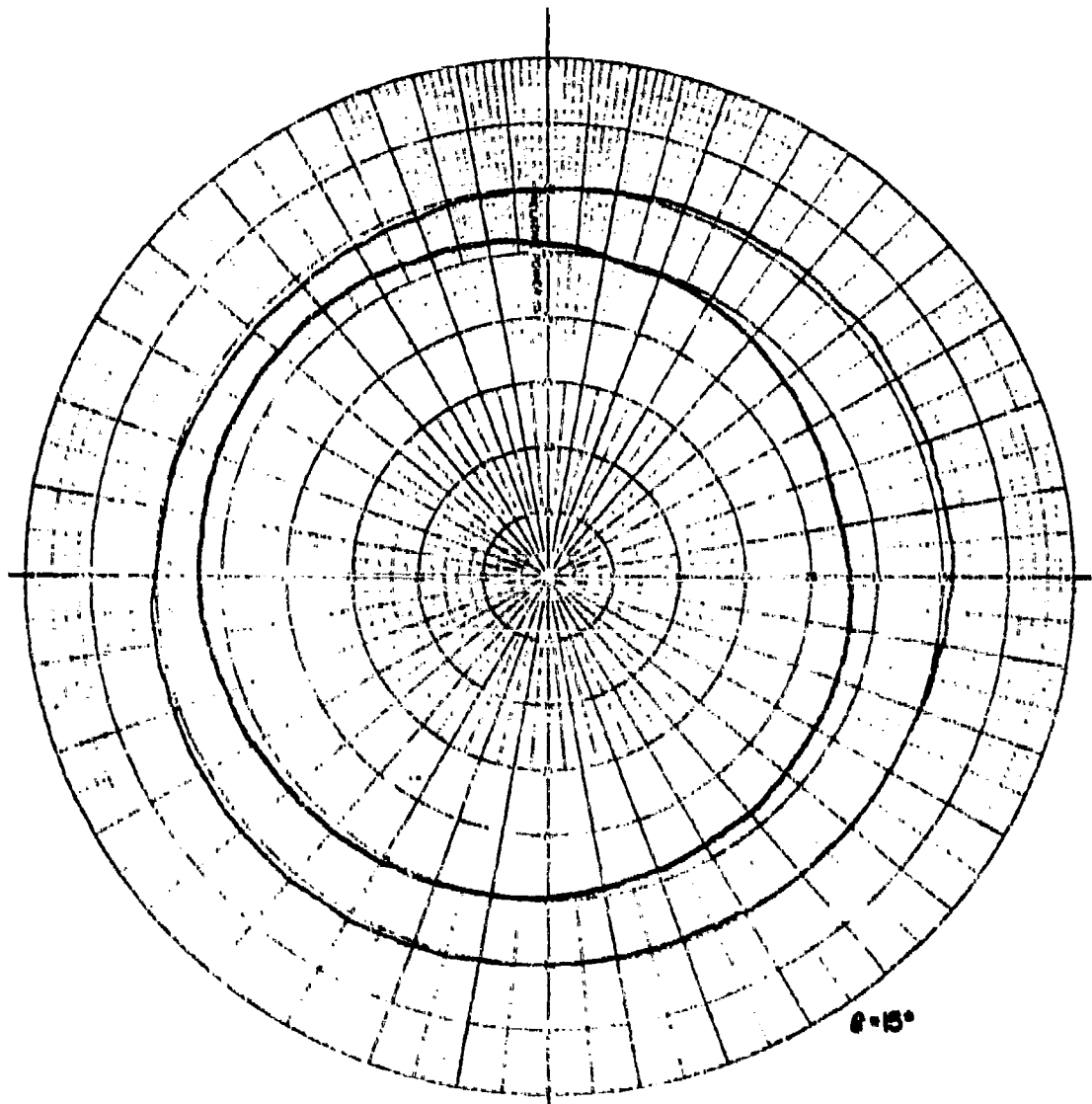


—— FIRST MODE PATTERN (A)  
 - - - - SECOND MODE PATTERN (B)

$f_0 = 1022$  mc - LEFT CIRCULAR POLARIZATION

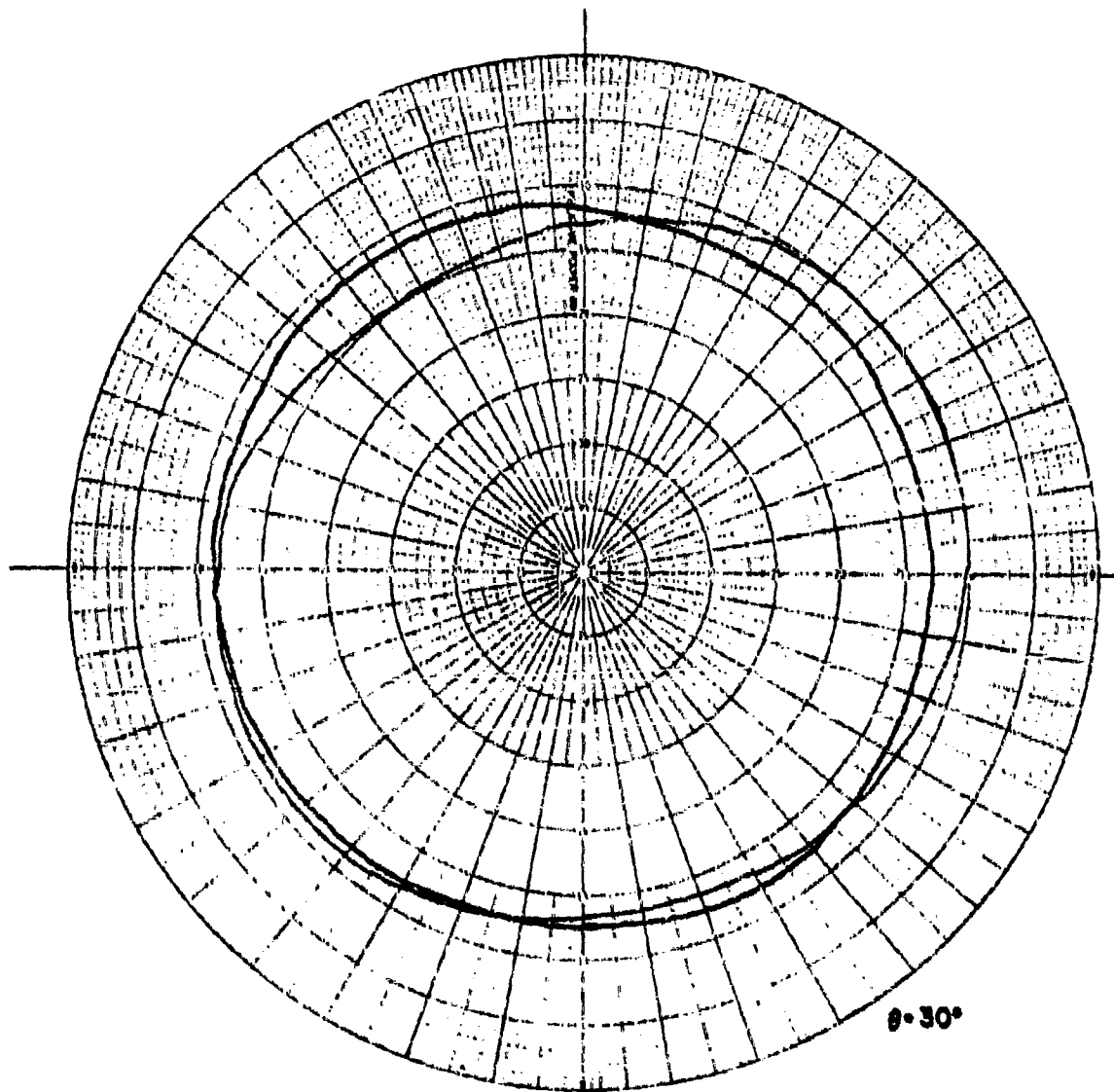
THESE PATTERNS WERE RECORDED AT A GAIN  
 SETTING 10.5 BELOW THE OTHERS

Figure 16. Azimuthal plots of A and B for  $\theta = 10^\circ$ .



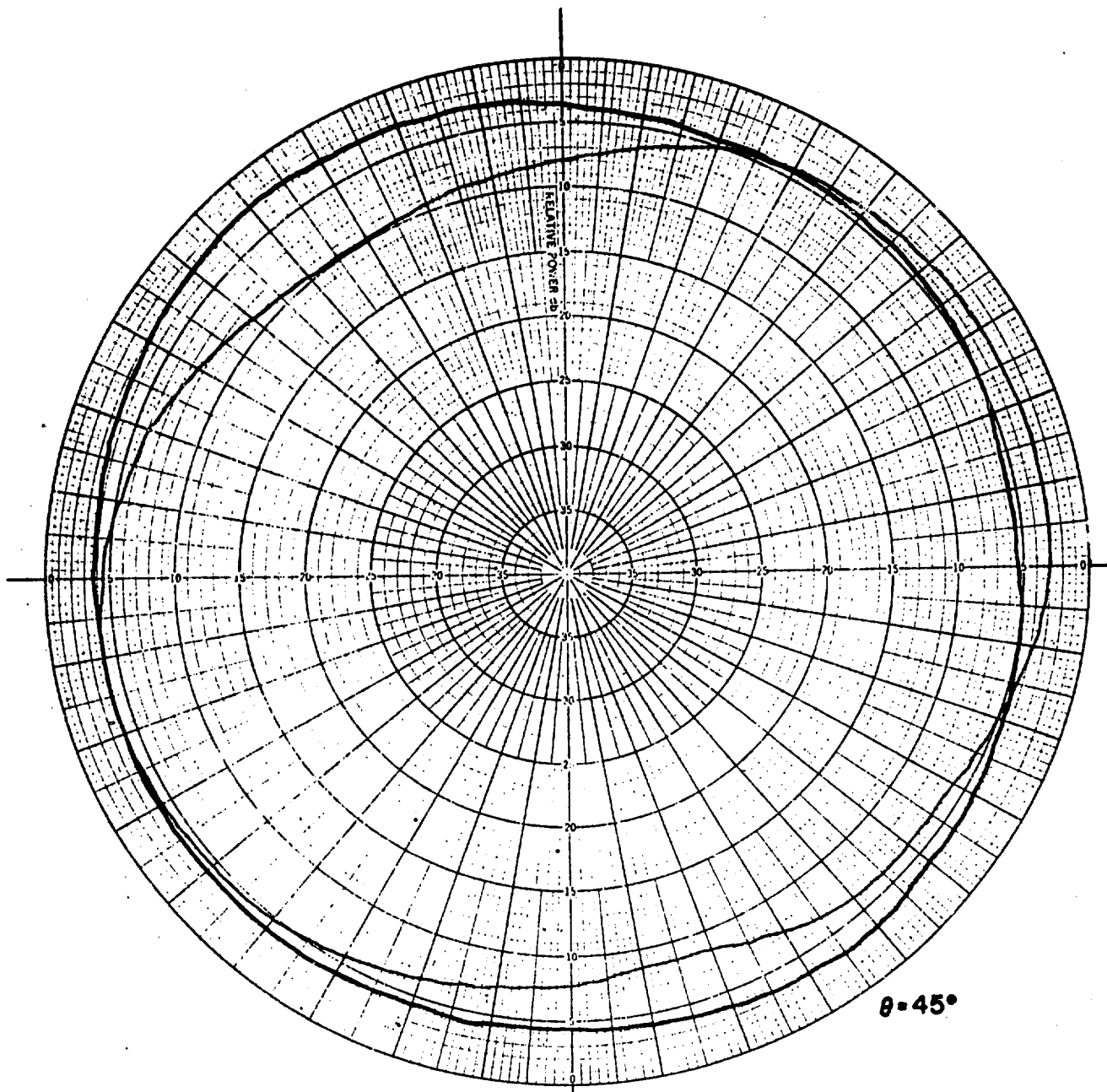
— FIRST MODE PATTERN (A)  
 - - - SECOND MODE PATTERN (B)  
 $f_0 = 1022$  MHz - LEFT CIRCULAR POLARIZATION  
 THESE PATTERNS WERE RECORDED AT A GAIN  
 SETTING 10dB BELOW THE OTHERS

Figure 17. Azimuthal plots of A and B for  $\theta = 15^\circ$



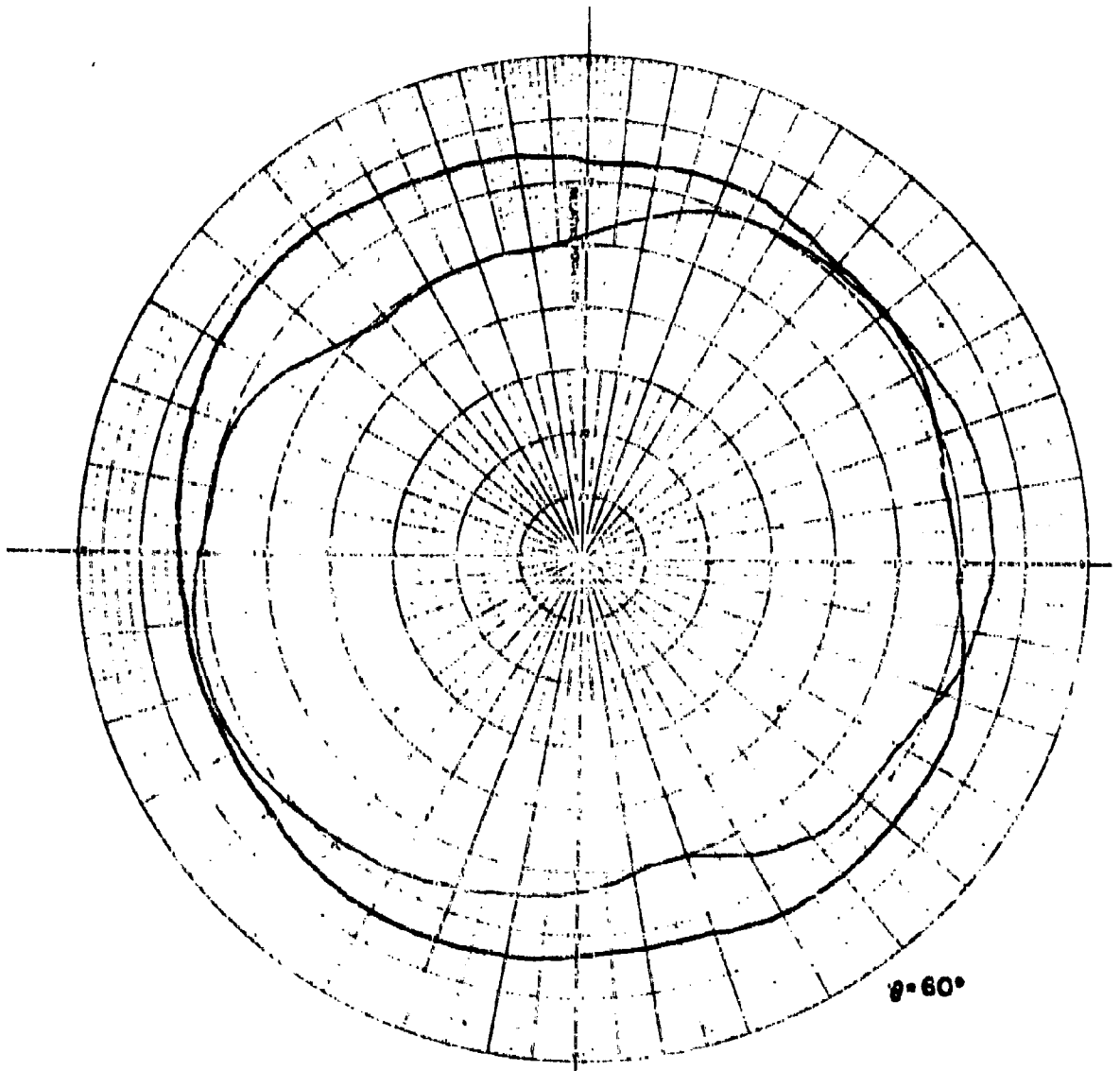
——— FIRST MODE PATTERN (A)  
 - - - SECOND MODE PATTERN (B)  
 $f_0 = 1022$  mc - LEFT CIRCULAR POLARIZATION  
 THESE PATTERNS WERE RECORDED AT A GAIN  
 SETTING 10db BELOW THE OTHERS

Figure 18. Azimuthal plots of A and B for  $\theta = 30^\circ$ .



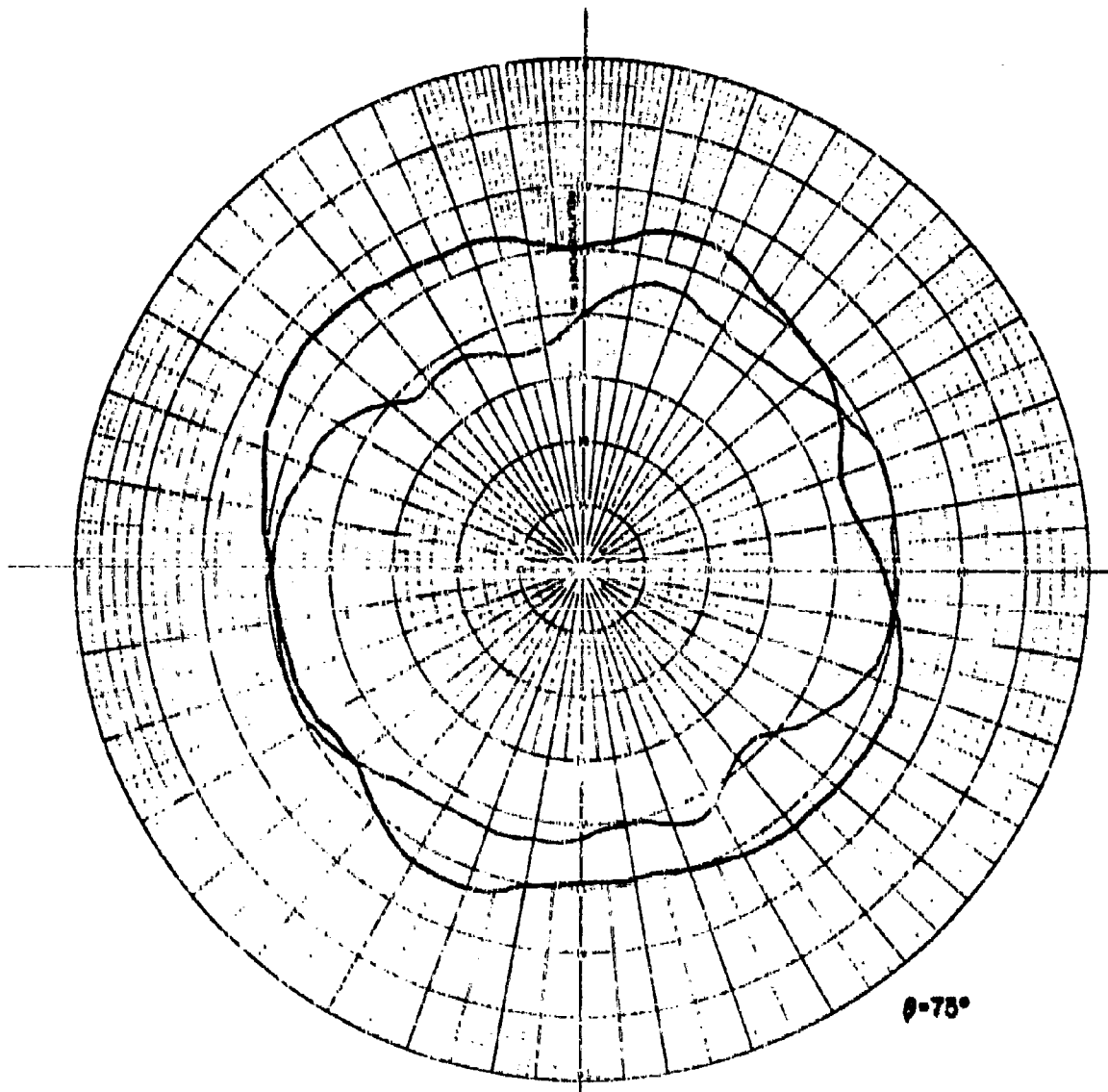
——— FIRST MODE PATTERN (A)  
 - - - SECOND MODE PATTERN (B)  
 $f_0 = 1022$  mcs - LEFT CIRCULAR POLARIZATION

Figure 19. Azimuthal plots of A and B for  $\theta = 45^\circ$ .



— FIRST MODE PATTERN (A)  
 - - - SECOND MODE PATTERN (B)  
 $f_0 = 1022$  mcs - LEFT CIRCULAR POLARIZATION

Figure 20. Azimuthal plots of A and B for  $\theta = 60^\circ$ .



——— FIRST MODE PATTERN (A)  
 - - - SECOND MODE PATTERN (B)  
 $f_0 = 1022$  mcs - LEFT CIRCULAR POLARIZATION

Figure 21. Azimuthal plots of A and B for  $\theta = 75^\circ$ .

#### 4. CONCLUSIONS AND RECOMMENDATIONS

Since data given in figures 8 through 21 indicate that the system behaves approximately as assumed in the formulation tabulated in table 2, it is assumed that the antenna can be used to determine the spherical coordinate angles  $\phi$  and  $\theta$ . It is estimated that the determination of  $\theta$  will be most precise for  $15^\circ < \theta < 75^\circ$ .

No attempts have been made to optimize the circuit and antenna. However, it has been demonstrated<sup>1</sup> that the spiral antenna is a precise phasing device, suggesting the possibility of engineering an accurate direction finder. Ultimate system accuracy will also be a function of the frequency dependence and losses of the processing networks. One source of azimuth error is discussed in appendix A.

Investigation of the three arrangements listed below may provide a method of increasing the precision of the direction finder.

(1) Increasing the  $\lambda/4$  spacing between the antenna and the ground plane, causing a partial null in the first mode radiation pattern.

(2) Adding a similar antenna element in front of the antenna, increasing the gain of both first and second modes.

(3) Adding an antenna for the first mode only in front of the spiral antenna, thus increasing the first mode gain only.

No attempt has been made up to this time to evaluate the relative efficacy of the various arrangements.

---

<sup>1</sup>J. A. Kaiser, "The Archimedean Two-Wire Spiral Antenna," IRE PGAP, Vol. AP-8 (1960).

## APPENDIX A

### FREQUENCY ERROR ANALYSIS

One possible source of error in the spiral antenna direction finder is the effect of a change in frequency from the design value. If the antenna is used as a direction finder, a shift in the source frequency would cause lines e and f of the network to have lengths that differ by more or less than a quarter wavelength. Also, if the system is to be used to search for and locate unknown signal sources, it would be necessary to know over what frequency range the system can be designed to search without exceeding an acceptable error in the calculated direction.

Equations (1) are rewritten for ease of analysis, as

$$\phi = \tan^{-1} \left[ \frac{E-F}{C-D} \right]$$

and

$$\theta = \tan^{-1} \left[ \left( \frac{A}{B} \right)^{1/2} \tan \theta_0 \right]$$

The only arms affected by a shift in frequency are E and F, so that the observed elevation angle is not affected by a change in frequency. If the difference in line length is equivalent to an angular rotation of  $\gamma$  degrees, then the input signals to arms E and F can be written (neglecting  $e^{j\omega t}$ ) as

$$E: (\alpha \sin \theta e^{j2\phi} + \beta \cos \theta e^{j\phi}) e^{-j\gamma} \\ + \alpha \sin \theta e^{j2\phi} + \beta \cos \theta e^{j\phi}$$

$$F: (\alpha \sin \theta e^{j2\phi} + \beta \cos \theta e^{j\phi}) e^{-j\gamma} \\ - (-\alpha \sin \theta e^{j2\phi} - \beta \cos \theta e^{j\phi})$$

For square law detection, the output of E is proportional to

$$\alpha^2 \sin^2 \theta (1 - \cos \gamma) + \beta^2 \cos^2 \theta (1 + \cos \gamma) + 2 \alpha \beta \sin \theta \cos \theta \sin \phi \sin \gamma$$

and the output of F is proportional to

$$\alpha^2 \sin^2 \theta (1 + \cos \gamma) + \beta^2 \cos^2 \theta (1 - \cos \gamma) - 2 \alpha \beta \sin \theta \cos \theta \sin \phi \sin \gamma$$

Thus the observed value of  $\phi$  (call it  $\phi'$ ) is found to be

$$\begin{aligned}\phi' &= \tan^{-1} \left[ \frac{E - F}{C - D} \right] \\ &= \tan^{-1} \left[ \frac{(\beta^2 \cos^2 \theta - \alpha^2 \sin^2 \theta) \cos \gamma + 2 \alpha \beta \sin \theta \cos \theta \sin \phi \sin \gamma}{2 \alpha \beta \sin \theta \cos \theta \cos \phi} \right] \\ &= \tan^{-1} \left[ \left( \frac{\beta^2 \cos^2 \theta - \alpha^2 \sin^2 \theta}{2 \alpha \beta \sin \theta \cos \theta} \right) \frac{\cos \gamma}{\cos \phi} + \tan \phi \sin \gamma \right]\end{aligned}$$

The error  $\phi' - \phi$  is thus

$$\phi' - \phi = \tan^{-1} \left[ \left( \frac{\beta^2 \cos^2 \theta - \alpha^2 \sin^2 \theta}{2 \alpha \beta \sin \theta \cos \theta} \right) \frac{\cos \gamma}{\cos \phi} + \tan \phi \sin \gamma \right] - \phi$$

The error in azimuth angle is seen to be strongly dependent upon the elevation angle  $\theta$ .

Substituting the crossover point relation

$$\alpha \sin \theta_0 = \beta \cos \theta_0$$

gives, after some rearrangement

$$\phi' - \phi = \tan^{-1} \left[ \left( \frac{\tan^2 \theta_0 - \tan^2 \theta}{2 \tan \theta_0 \tan \theta} \right) \frac{\cos \gamma}{\cos \phi} + \tan \phi \sin \gamma \right] - \phi$$

If the gains of the first and second modes are equal ( $\tan \theta_0 = 1$ ), this reduces to

$$\phi' - \phi = \tan^{-1} \left[ \frac{\cot 2\theta \cos \gamma}{\cos \phi} + \tan \phi \sin \gamma \right] - \phi$$

Thus, for elevation angles ( $\theta$ ) near  $0^\circ$  (on axis) or near  $90^\circ$  (in the plane of the spiral array), a large error in the calculated value of  $\phi$  may occur for values of  $\gamma \pm \pi/2$ .

Plotting the error in azimuthal angle as a function of  $\gamma$ , as shown in figures A1 and A2, reveals that the maximum error occurs at values of  $\phi$  near  $0^\circ$ , and the possible error increases greatly with increasing deviation of the line length difference from  $90^\circ$ . If this device is to be used to locate unknown signal sources, it is desirable to have a single device operate over a wide range of frequencies. By using newly

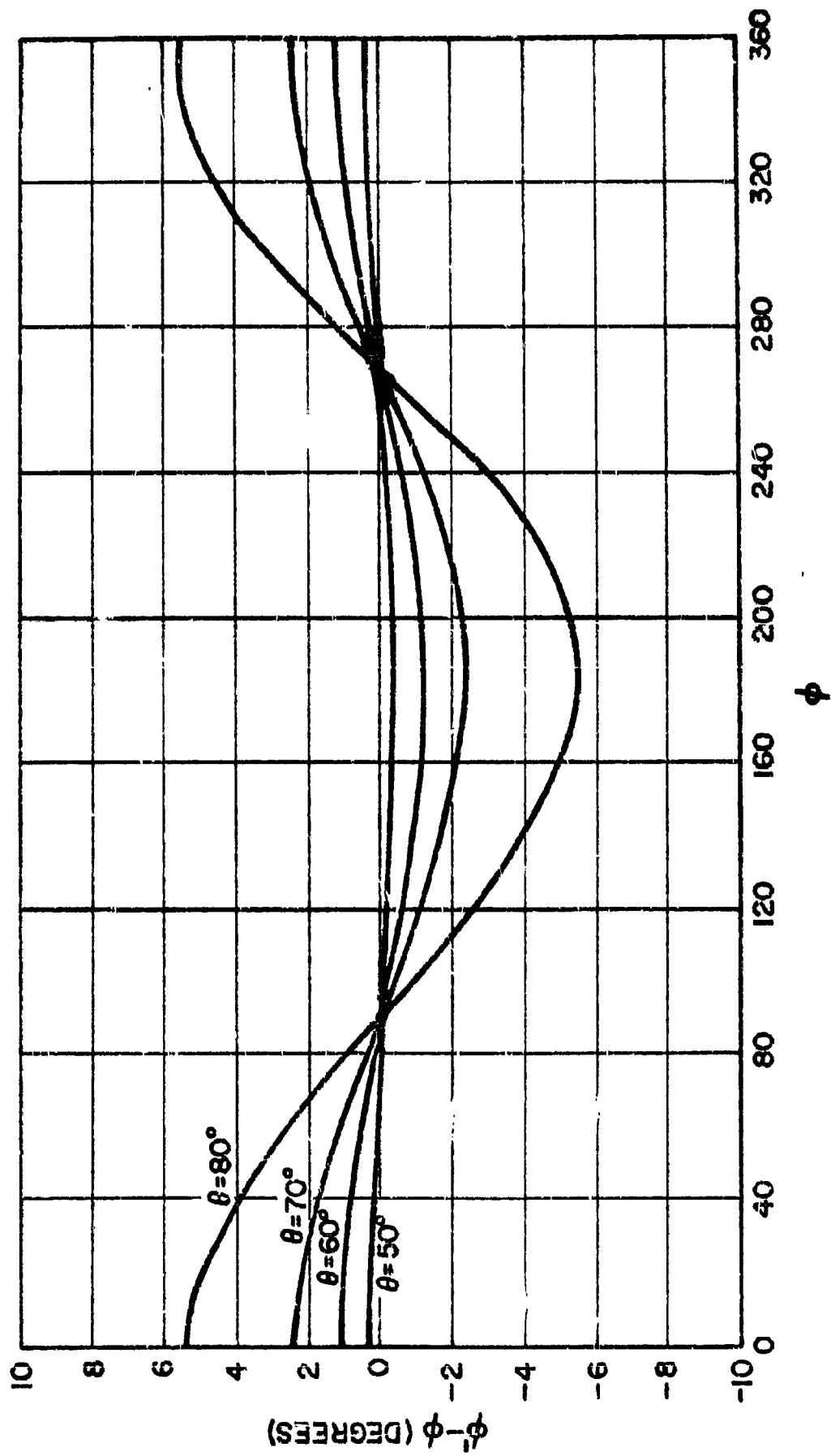


Figure A1. Theoretical azimuthal error for  $\gamma = 92^\circ$ .

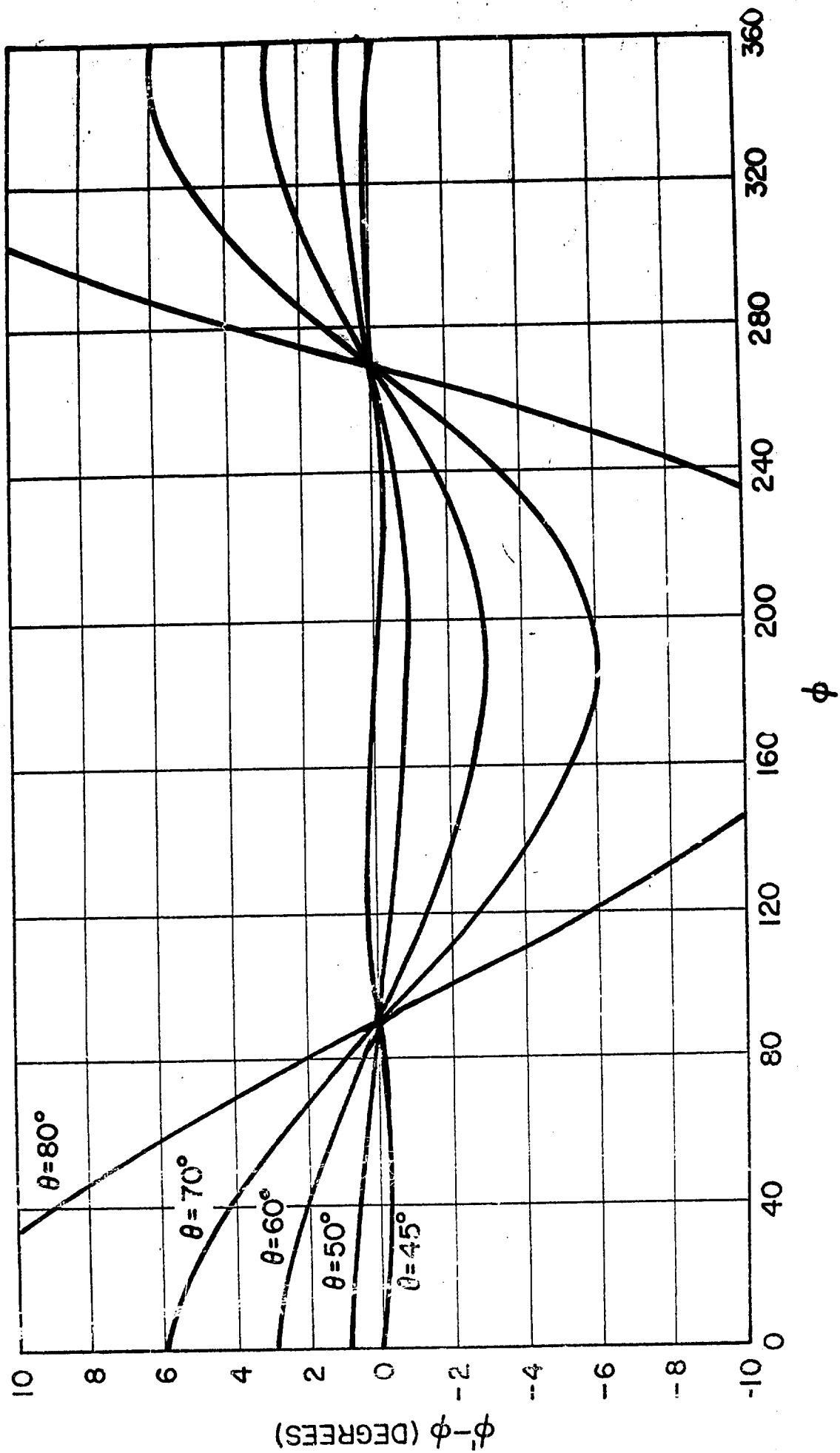


Figure A2. Theoretical azimuth error for  $\gamma = 95^\circ$ .

developed<sup>1</sup> phase shifters, in which the phase difference between two channels is very nearly  $90^\circ$  over a broad frequency range, it is theoretically possible to hold  $\gamma$  to the range of  $88^\circ$  to  $92^\circ$  over a 2:1 range in frequency. Assuming that this value can be approximately held in practice and that other sources of error do not exist, the maximum error in calculated azimuthal angle for elevation angles between  $10^\circ$  and  $80^\circ$  is held to approximately  $5^\circ$ .

---

<sup>1</sup>"A New Class of Broad-Band Microwave 90-Degree Phase Shifters,"  
B. M. Schiffman, IRE Trans Vol MTT-6 pp 232-237, 1958.

**DISTRIBUTION**

Office of the Director of Defense Research & Engineering  
The Pentagon, Washington 25, D. C.  
Attn: Technical Library (Rm 3E1065) - 2 copies

Department of the Army  
Office of the Chief Ordnance  
The Pentagon, Washington 25, D. C.  
Attn: ORDTN (Nuclear & Special Components Br)  
Attn: ORDTU (GM Systems Br)  
Attn: ORDTB (Research Br)  
Attn: ORDTW (Artillery & Vehicle Systems Br)

Office of the Chief of Research & Development  
Department of the Army  
Washington 25, D. C.  
Attn: Director, Army Research Office  
Attn: Director, Special Weapons

Commanding General  
Army Ballistic Missile Agency  
Redstone Arsenal, Alabama  
Attn: ORDAB-DG, Director  
Attn: ORDAB-DGI  
Attn: Technical Documents Library

Commanding General  
U.S. Army Ordnance Missile Command  
Redstone Arsenal, Alabama  
Attn: ORDXR-O, Research Div  
Attn: ORDXR-R, R&D Div  
Attn: R&D Director, Future Missile Systems Div  
Attn: Col. C. W. Gustafson, Combat Req Br.  
Attn: Capt. W. Allan, Exp Programs Br.  
Attn: D. Salonimer, Exp Programs Br.  
Attn: Technical Documents Library

Commanding General  
Aberdeen Proving Ground, Maryland  
Attn: BRL—Weapons Systems Laboratory

Commanding General  
Ordnance Special Weapons-Ammunition Command  
Dover, New Jersey

Commanding Officer  
Picatinny Arsenal  
Dover, New Jersey  
Attn: Library

PRECEDING PAGE BLANK

**DISTRIBUTION (Continued)**

Commanding Officer  
U.S. Army Signal Research & Development Laboratory  
Fort Monmouth, New Jersey  
Attn: Surveillance Dept.  
Attn: Technical Library  
Attn: Nathan Lipetz SIGRA/EL-FEE

Ordnance Technical Intelligence Agency  
Arlington Hall Station  
Arlington 12, Virginia

Commanding General  
Engineer Research & Development Laboratories  
U.S. Army  
Fort Belvoir, Virginia

Department of the Navy  
Bureau of Ships  
Washington 25, D. C.  
Attn: Mr. Leo V. Cumina, Rm 3349, Main Navy Bldg.

Commander  
Naval Research Laboratory  
Washington 25, D. C.  
Attn: Dr. A. E. Marston, Code 5200

Commander  
Aeronautical Systems Div  
Wright-Patterson Air Force Base, Ohio  
Attn: Mr. George F. Duree, WWDPVX-1

Commander  
Rome Air Development Center  
Griffiss Air Force Base, New York  
Mr. Patsy A. Romanelli, RCLRA-2

Commander  
Armed Services Technical Information Agency  
Arlington Hall Station  
Arlington 12, Virginia  
Attn: TIPDR (10 copies)

Department of Commerce  
Technical Services  
Technical Reports Section  
Washington 25, D. C.

**DISTRIBUTION (Cont'd)**

U.S. Library of Congress  
Washington 25, D. C.  
Attn: Science & Technology Division

National Bureau of Standards  
Washington 25, D. C.

Commander  
Air Force Research Division  
L O Hanscom Field  
Bedford, Mass  
Attn: Charles E. Ellis, Jr., CRNDM

National Aeronautics and Space Administration  
Goddard Space Flight Center  
Greenbelt, Maryland  
Attn: J. A. Kaiser, Code 525  
Bldg 3, Room 70 - 8 copies

**INTERNAL DISTRIBUTION**

Horton, B. M./McEvoy, R. W., Lt. Col.  
  Apstein, H./Gewirtz, H. L./Guarino, P. A./Kalmus, H. P.  
  Schwenk, C. C.  
Hardin, C. D., Lab 100  
Sommer, R, Lab 200  
Hatcher, R. D., Lab 300  
Landis, P. E., Lab 400  
Nilson, H., Lab 500  
Flyer, I. N., Lab 600  
Campagna, J. H./Apolenis, C. J., Div 700  
Demasi, R., Div 800  
Franklin, P. J./Horsley, E. F., Lab 900  
Seaton, J. W., 260  
Tozzi, L.M., 210  
Haas, P., 230  
Griffin, P. W., 240  
Pepper, W. H., 260 - 8 copies  
Little, J., 250 - 8 copies  
Cunco, J. V., 240  
Rotkin, I., 002  
Eichberg, R. L., 800  
Bryant, W. T., 520  
Distad, M. F., 100  
Epstein, A. M., 510  
Kalmus, H. P., 002  
Godfrey, T. B., 310  
McCoskey, R. E., 230  
Witte, J. J., 310  
Moorhead, J. G., 310  
Technical Reports Unit, 800  
Technical Information Office, 010 - 10 copies  
DOFL Library - 5 copies

(Two pages of abstract cards follow)

AD

Accession No.

Automatic direction finder—  
Miniaturization

Diamond Ordnance Fuze Laboratories, Washington 25, D. C.  
A MINIATURE AUTOMATIC DIRECTION FINDER - E. B. Smith, Jr.,  
J. A. Kaiser, V. H. Pepper, J. Little  
TR-1031, 14 May 1962, 14 pp text, 24 illus. Department of the  
Army DA-3906-01-013, OMS 521011.17500, DOWF Proj 26100  
UNCLASSIFIED REPORT

A miniaturized unambiguous direction finder with no moving parts is described. At a frequency of 1000 Mc, a complete system, consisting of a two-wire spiral antenna, with cavity backing, operating in the first two radiation modes can be built into a cylinder 10 in. in diameter and 3 in. deep. Direct scaling laws apply, so that at 3000 Mc, for example, the cylinder would be 3 in. in diameter and 1 1/2 in. deep. Since there are no moving parts, and printed-circuit techniques can be used, the total weight (excluding power supply and readout or display) will be less than 1/3 lb. The pattern of this antenna array gives hemispheric coverage. The output, fed into an analog device, gives a determination of the elevation and azimuth of a received signal, with no ambiguity, in the hemisphere bounded by the plane of the spiral. The processing network consists of two 3-way power dividers and a pair of hybrids, which can be mounted on the back of the cavity by using strip-line techniques. An experimental version of the system has been built and preliminary data are presented.

AD

Accession No.

Automatic direction finder—  
Miniaturization

Diamond Ordnance Fuze Laboratories, Washington 25, D. C.  
A MINIATURE AUTOMATIC DIRECTION FINDER - E. B. Smith, Jr.,  
J. A. Kaiser, V. H. Pepper, J. Little  
TR-1031, 14 May 1962, 14 pp text, 24 illus. Department of the  
Army DA-3906-01-013, OMS 521011.17500, DOWF Proj 26100  
UNCLASSIFIED REPORT

A miniaturized unambiguous direction finder with no moving parts is described. At a frequency of 1000 Mc, a complete system, consisting of a two-wire spiral antenna, with cavity backing, operating in the first two radiation modes can be built into a cylinder 10 in. in diameter and 3 in. deep. Direct scaling laws apply, so that at 3000 Mc, for example, the cylinder would be 3 in. in diameter and 1 1/2 in. deep. Since there are no moving parts, and printed-circuit techniques can be used, the total weight (excluding power supply and readout or display) will be less than 1/3 lb. The pattern of this antenna array gives hemispheric coverage. The output, fed into an analog device, gives a determination of the elevation and azimuth of a received signal, with no ambiguity, in the hemisphere bounded by the plane of the spiral. The processing network consists of two 3-way power dividers and a pair of hybrids, which can be mounted on the back of the cavity by using strip-line techniques. An experimental version of the system has been built and preliminary data are presented.

AD

Accession No.

Automatic direction finder—  
Miniaturization

Diamond Ordnance Fuze Laboratories, Washington 25, D. C.  
A MINIATURE AUTOMATIC DIRECTION FINDER - E. B. Smith, Jr.,  
J. A. Kaiser, V. H. Pepper, J. Little  
TR-1031, 14 May 1962, 14 pp text, 24 illus. Department of the  
Army DA-3906-01-013, OMS 521011.17500, DOWF Proj 26100  
UNCLASSIFIED REPORT

A miniaturized unambiguous direction finder with no moving parts is described. At a frequency of 1000 Mc, a complete system, consisting of a two-wire spiral antenna, with cavity backing, operating in the first two radiation modes can be built into a cylinder 10 in. in diameter and 3 in. deep. Direct scaling laws apply, so that at 3000 Mc, for example, the cylinder would be 3 in. in diameter and 1 1/2 in. deep. Since there are no moving parts, and printed-circuit techniques can be used, the total weight (excluding power supply and readout or display) will be less than 1/3 lb. The pattern of this antenna array gives hemispheric coverage. The output, fed into an analog device, gives a determination of the elevation and azimuth of a received signal, with no ambiguity, in the hemisphere bounded by the plane of the spiral. The processing network consists of two 3-way power dividers and a pair of hybrids, which can be mounted on the back of the cavity by using strip-line techniques. An experimental version of the system has been built and preliminary data are presented.

AD

Accession No.

Automatic direction finder—  
Miniaturization

Diamond Ordnance Fuze Laboratories, Washington 25, D. C.  
A MINIATURE AUTOMATIC DIRECTION FINDER - E. B. Smith, Jr.,  
J. A. Kaiser, V. H. Pepper, J. Little  
TR-1031, 14 May 1962, 14 pp text, 24 illus. Department of the  
Army DA-3906-01-013, OMS 521011.17500, DOWF Proj 26100  
UNCLASSIFIED REPORT

A miniaturized unambiguous direction finder with no moving parts is described. At a frequency of 1000 Mc, a complete system, consisting of a two-wire spiral antenna, with cavity backing, operating in the first two radiation modes can be built into a cylinder 10 in. in diameter and 3 in. deep. Direct scaling laws apply, so that at 3000 Mc, for example, the cylinder would be 3 in. in diameter and 1 1/2 in. deep. Since there are no moving parts, and printed-circuit techniques can be used, the total weight (excluding power supply and readout or display) will be less than 1/3 lb. The pattern of this antenna array gives hemispheric coverage. The output, fed into an analog device, gives a determination of the elevation and azimuth of a received signal, with no ambiguity, in the hemisphere bounded by the plane of the spiral. The processing network consists of two 3-way power dividers and a pair of hybrids, which can be mounted on the back of the cavity by using strip-line techniques. An experimental version of the system has been built and preliminary data are presented.

REMOVAL OF EACH CARD WILL BE NOTED ON INSIDE BACK COVER, AND REMOVED CARDS WILL BE TREATED AS REQUIRED BY THEIR SECURITY CLASSIFICATION.